Powering the Rijksrederij fleet with green methanol fuel cells

MSc thesis

As part of the degree of Master of Science in Marine Technology
at the Delft University of Technology.

24/02/2022

Student / author:	D. Pluijlaar
Supervisor TU Delft:	Dr. Ir. L. van Biert
Supervisor Rijkswaterstaat:	Ir. L. Verheijen
Chairman Graduation Committee:	Dr. Ir. K. Visser

TU Delft

Rijkswaterstaat
Ministry of Infrastructure and Water Management

Thesis for the degree of MSc in Marine Technology in the specialization of Marine Engineering

Powering the Rijksrederij fleet with green methanol fuel cells

By

Dion Pluijlaar

Performed at

Rijksrederij

This thesis MT.21/22.021.M is classified as confidential in accordance with the general conditions for projects performed by the TUDelft.

24 February 2022

Supervisors
Company supervisor: Ir. L. Verheijen
E-mail: loek.verheijen@rws.nl
TU Delft supervisor: Dr. Ir. L. van Biert
E-mail: l.vanbiert@tudelft.nl

Thesis exam committee
Chair/Responsible Professor: Ir. K. Visser
Staff Member: Dr. Ir. L. van Biert
Staff Member: Dr. Ir. R.D. Geertsma
Company Member: Ir. L. Verheijen

Author Details
Studynumber: 4287355
Author contact e-mail: dionpluijlaar@gmail.com

Summary

This research was performed with the goal of giving insight if the Rijksrederij is able to operate part of their fleet on renewable methanol and fuel cells, in order to work towards their goal of operating with net zero CO_2 emissions by 2030. This prompted a research question that focussed on both the renewable methanol supply and the technical implementation on board of some of the ships operated by the Rijksrederij.

First, multiple possible pathways for renewably producing methanol were considered. Three main pathways were identified: two of which using waste biomass, one using recycled CO_2 from on-board carbon capture. Green hydrogen could be provided using excess wind energy from Rijkswaterstaat's own wind parks. In a later stage, it was found that a combination of biomass derived CO_2 and recycled CO_2 would be most beneficial to use in the methanol production process, by hydrogenating the CO_2 with the beforementioned green hydrogen. However, this process resulted in net well-to-tank CO_2 emissions.

To gain insight in all necessary components, a literature study was performed on maritime fuel cell systems and methanol reformers. Next, a model based on these systems was constructed that could be used in two ways: to aid in selecting specific systems and tank dimensions to be installed on board of ships, and to calculate tank-to-propeller CO_2 emissions on both trip basis and yearly. Three different Rijksrederij ships were analysed using this model, and the spatial system integration on board was considered. In order to recycle the CO_2 to produce green methanol, an on-board carbon capture system was needed and also modelled. The model is parametric in a way that allows for other ship types and fuel cell related systems to be used as input. In the end, the tank-to-propeller emissions for the three ship types were calculated, and these findings could be extended towards a larger part of the Rijksrederij fleet in order to calculate the entire well-to-propeller emissions of this fleet.

It was found that there were net positive emissions stemming from two sources: the aforementioned methanol production related emissions, and the slip stemming from uncaptured CO_2 on board. Since not 100% of all CO_2 could be captured on board, this also results in a gap in available CO_2 for methanol production. In this sense, the production CO_2 gap and the net well-to-tank emissions go hand in hand, and eliminating the net emissions (by capturing CO_2 elsewhere, or improving the capture rate) also reduces the production gap. To achieve this, more research will be necessary.

Contents

1. Introduction

Human activities since the start of the industrial age have resulted in a 1°C rise in global temperature, with a current increase of 0.2°C every decade (Allen et al., 2018). The Paris agreement pushed nations to take action in order to limit the post-industrial temperature increase to well under 2°C, preferably to 1.5°C (UNFCCC, n.d.). Since the emission of greenhouse gases is the main contributor to global warming, the Netherlands adopted a climate law (*Klimaatwet*) with emission reduction targets based on the emission levels of 1990. To conform to this law, the Netherlands needs to emit 49% fewer greenhouse gases by 2030, and up to 95% fewer emissions by 2050. The Dutch Ministry of Transport and Water Management (*Ministerie van Infrastructuur en Waterstaat* or *IenW*) aims to be an inspiring frontrunner and has set its own target to be completely carbon neutral by 2030 (Ministerie van Infrastructuur en Waterstaat, 2020).

As the executive agency of IenW, Rijkswaterstaat also aims to eliminate its net carbon dioxide (CO_2) emissions by 2030. The Rijksrederij is a semi-independent subsidiary of Rijkswaterstaat and manages, maintains, and mans 100 vessels for various Dutch governmental bodies. These bodies include Rijkswaterstaat itself, the coast guard (*Kustwacht*), customs (*Douane*), and the Ministry of Agriculture, Nature and Food Quality. The fleet features both sea-going and inland vessels, all equipped for various different tasks. Tasks include marking of shipping lanes (placing and maintaining buoys), inspection and law enforcement, and measuring and research. Most vessels currently run on diesel (EN590), though ten of the multipurpose vessels (MPVs) run on biodiesel (B30). One of the largest sea-going ships in the fleet, fishery research vessel Tridens, as well as emergency towing vessels Guardian and Alp Ace, are currently the only vessels to operate on marine gas oil (MGO). In 2016, the fleet operated by the Rijksrederij amounted for about 44% of the total CO_2 emitted by Rijkswaterstaat. Several emission reduction measures are already in place, such as the use of biofuel blended into regular bunker fuels and changes in operational strategies. However, more severe measures are needed to further reduce the carbon footprint.

The Rijksrederij has taken an interest in the use of green methanol on board of their fleet. Not only can methanol reduce the overall CO_2 emissions, it also practically eliminates sulphur oxide emissions as methanol does not contain sulphur compounds. Nitrogen-based emissions – inherent to high temperature combustion - are also eliminated when methanol is used in fuel cells. Fuel cells also provide the possibility for more silent and efficient operation (Tronstad et al., 2017), and could be combined with a carbon capture system as CO_2 can be directly captured from methanol reformers (Wermuth, Zelenka, et al., 2020).

Fuel cells require hydrogen (H_2) as a fuel, which would also be an interesting option to the Rijksrederij. However, using methanol as a carrier of hydrogen and reforming it to hydrogen on-board has a clear advantage in terms of volumetric energy density and ease of storage. Sailing on methanol – both in internal combustion engines and fuel cells – still leads to emission of (carbon-based) greenhouse gases (GHG). The question is how much the total (so called) well-to-propeller emissions can be reduced if the switch to renewable methanol in fuel cells is made. Renewable sources of both the hydrogen and carbon parts of methanol must be investigated.

1.1. Problem statement

The Rijksrederij has taken an interest in using renewable methanol and fuel cells on their fleet. However, since (reforming of) methanol still results in CO_2 emissions, it is currently not possible to reach the goal of operating carbon neutral in 2030 – even when renewable methanol is used. Therefore, alternative measures need to be investigated to eliminate the emissions of greenhouse gases such as CO_2, in other words make the total (well-to-propeller) emissions of renewable methanol fuel net zero.

1.2. Research question and report structure

This thesis revolves around answering the main research question:

"To what extent can fuel cells and renewable methanol be used to eliminate the well-to-propeller greenhouse gas emissions of the Rijksrederij fleet?"

To answer this question, it will be broken down into three sub questions. First, the well-to-propeller emissions are split into well-to-tank and tank-to-propeller emissions and considered separately, the former being investigated in Chapter 2, which considers the first sub question:

1. *What pathways using Rijkswaterstaat's own resources can be used to produce renewable methanol in order to reduce or eliminate the well-to-tank greenhouse gas emissions?*

This sub question concerns the feedstock availability and the associated greenhouse gas emissions if these feedstocks are used to produce methanol. How this methanol can be used in fuel cell systems on board of ships is discussed in Chapter 3, which is based on literature. The technical workings of all systems related to methanol fuel cells (including reformers, optional carbon capture systems and tank sizes) are modelled using MATLAB-Simulink in order to be able to calculate the tank-to-propeller emissions based on various ship parameters, including operational profile. An explanation of the various sub models is given in Chapter 4. The sub question that is answered by constructing this model is as follows:

2. *How can the tank-to-propeller greenhouse gas emissions of a methanol fuel cell powered ship be calculated?*

In another step towards answering the main research question, several ships of the Rijksrederij are investigated in their ability to be outfitted with methanol fuel cell systems and carbon capture systems. The spatial integration (using output parameters from the previously constructed model) is considered when answering the third sub question in Chapter 5:

3. *How can methanol fuel cells and a carbon capture system be integrated into a Rijksrederij ship?*

Following the system integration, the model is again used to calculate the tank-to-propeller emissions of the selected ships. This is done in Chapter 6. Finally, the main research question can be answered in Chapter 7. As this research question involves a greater part of the Rijksrederij fleet than those that are considered in the third sub question, the findings of the previous chapter need to be extended to this larger fleet. The total well-to-propeller emissions of this fleet will be calculated (keeping in mind the various assumptions made in this thesis), and if the total emissions are positive, ways to further reduce or eliminate these emissions will be presented. In Chapter 8, conclusions will be presented along with a discussion on the various assumptions and constraints used in this thesis.

2. Well-to-tank

The first sub question is:

What pathways using Rijkswaterstaat's own resources can be used to produce renewable methanol in order to reduce or eliminate the well-to-tank greenhouse gas emissions?

In general, well-to-tank emissions include everything from gathering feedstocks to the production of methanol, up to the point where fuel is loaded into the ship. In this thesis, the emissions that are being analysed are the net CO_2 emissions stemming from the feedstocks themselves (such as growing biomass and producing hydrogen using wind energy), and the CO_2 emissions stemming from the production of methanol. Emissions related to harvesting feedstocks and transportation emissions are not considered in this analysis.

2.1. Available feedstocks

In exploring options for methanol production from within Rijkswaterstaat's resources, three main feedstock sources were identified: excess wind energy to produce hydrogen, waste biomass from mown grass as a carbon source, and recycled CO_2 from on-board carbon capture.

2.1.1. Excess wind energy

Rijkswaterstaat is set to start operating a 100 MW wind park in 2023. This wind park can generate over 400 GWh of green energy, which will be used to reach Rijkswaterstaat's goal of operating energy neutrally by 2030. An annual overproduction of 250 GWh is estimated. Until 2028, this overcapacity is available for other Dutch governmental bodies. After 2028, the overcapacity is available to Rijkwaterstaat again, and could be used to generate green hydrogen via electrolysis of water.

One kilogram of hydrogen contains 142 MJ or 39.4 kWh of energy. At 100% efficiency, electrolysis of water would require the same amount of energy to produce hydrogen. However, electrolysers are far from being 100% efficient, with an approximate 78% efficiency of current technology (including auxiliary processes) (Diéguez et al., 2008; NEL, 2020). With 250 GWh available annually, this would result in a total of just under 5000 tonnes of hydrogen:

$$m_{H_2} = \eta_{electrolyser} \cdot \frac{E_{available}}{HHV_{H_2}} = 78\% \cdot \frac{250 \cdot 10^6\ [\text{kWh}]}{39.4\ [\text{kWh/kg}]} = 4949 \cdot 10^3\ [\text{kg}] \qquad (2.1)$$

2.1.2. Waste biomass

One of Rijkswaterstaat's tasks is maintaining roads throughout the Netherlands. This includes mowing grass on roadsides, which produces waste grass biomass. Currently, Rijkwaterstaat is involved in a pilot project to produce biogas in a mono fermenter, which can be used in generators to provide heating and power to Rijkswaterstaat offices. A by-product of this mono fermenter is pure CO_2. This pure CO_2 could be used in methanol synthesis, as it would otherwise be emitted into the air. With the current projected biogas production, 3500 tonnes of CO_2 are produced annually.

2.1.3. Captured carbon dioxide

If CO_2 is captured using on-board carbon capture, it can be recycled into methanol (together with hydrogen). The implementation of these on-board systems will be discussed later in this thesis.

2.2. Available methanol production methods

Based on the available feedstocks, two main methanol production methods are explored. The most common (non-renewable) methanol synthesis process is from syngas, which can be derived from various carbon-containing sources, including natural gas, coal, and biomass. For renewable methanol, biomass can be used as feedstock for syngas, by using a gasification process. The second option explored in this section is CO_2 hydrogenation, which can be used to produce renewable methanol from pure H_2 and CO_2 feedstocks.

2.2.1. Methanol synthesis via syngas

The most common process of synthesising methanol starts by producing a synthetic gas (syngas).

Syngas contains mostly H_2 and CO, but CO_2 can also be present due to the reverse water-gas shift reaction (Dalena et al., 2018). This syngas is fed to a methanol synthesis process. The conventional methanol synthesis loop is presented in Figure 1. The feed gas is optionally preheated and fed into a reactor, where the actual synthesis occurs. Since this is an exothermic reaction, the reactor needs cooling. The produced gas is also cooled to separate the liquid contents from unreacted gas. The separated liquid mostly consists of methanol, which needs further purification. The unreacted gas is fed back into the reactor, though a small part is purged to avoid too much inert gas being present in the feed (Dieterich et al., 2020).

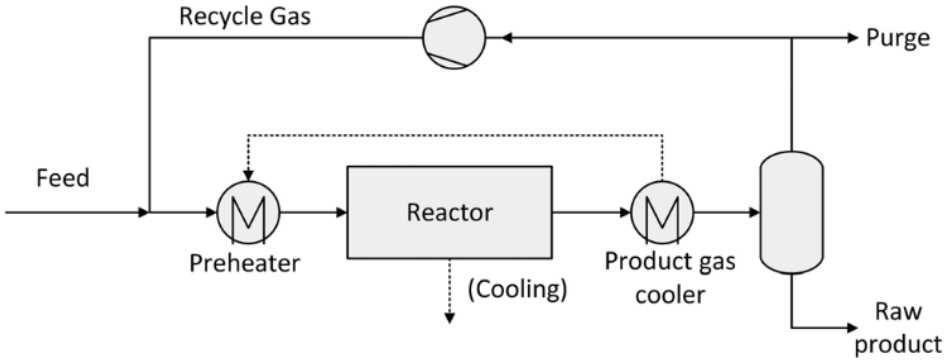

Figure 1: Simplified conventional methanol synthesis loop (Dieterich et al., 2020)

The composition of the syngas influences the ratio of gas that gets converted, indicated by the stoichiometric number. This number reflects the molar ratio of reactants. For syngas composition, it is calculated as follows (Bozzano & Manenti, 2016):

$$S = \frac{moles_{\mathrm{H_2}} - moles_{\mathrm{CO_2}}}{moles_{\mathrm{CO_2}} + moles_{\mathrm{CO}}} \tag{2.2}$$

Ideal conditions (where no CO_2 is present) dictate a stoichiometric number of 2, but due to the presence of CO_2 most commercial catalysts work optimally for values slightly higher than 2 (Bozzano & Manenti, 2016). This indicates a hydrogen excess, which is recycled into the feed gas. Methanol synthesis from carbon monoxide and carbon dioxide occur respectively via the following exothermic reactions (Blumberg et al., 2017):

$$\mathrm{CO} + 2\mathrm{H_2} \leftrightarrows \mathrm{CH_3OH} \tag{2.3}$$

$$\mathrm{CO_2} + 3\mathrm{H_2} \leftrightarrows \mathrm{CH_3OH} + \mathrm{H_2O} \tag{2.4}$$

From these reaction equations it can be seen why it is favourable to use syngas with a higher CO content: methanol synthesis from CO_2 requires more hydrogen as water is formed as by-product.

2.2.2. Hydrogenation of CO_2

The hydrogenation of CO_2 can be used to produce green methanol from renewable hydrogen and carbon dioxide. It involves the following main reaction:

$$CO_2 + 3H_2 \leftrightarrows CH_3OH + H_2O \quad (2.5)$$

Two side reactions also occur, the reverse water gas shift (RWGS) reaction and hydrogenation of carbon monoxide (Lee et al., 2020):

$$CO_2 + H_2 \leftrightarrows CO + H_2O \quad (2.6)$$

$$CO + 2H_2 \leftrightarrows CH_3OH \quad (2.7)$$

Although the reaction rate is improved with increased temperature, dictating at least 200 degrees Celsius (Atsbha et al., 2021), selectivity towards the methanol synthesis reaction (2.4) is higher at lower temperatures. Higher selectivity towards methanol synthesis is achieved by increasing the pressure, or by increasing the H_2/CO_2 ratio above the stoichiometric ratio of 2:1 (Stangeland et al., 2018). Typical catalysts are Cu/Al_2O_3 and $Cu/ZnO/Al_2O_3$ with Zr modifiers (Degnan, 2017). Atsbha et al. (2021) gives an extensive overview of research on different catalysts for both the methanol synthesis and RWGS reactions.

Green methanol production has been commercially operative since 2012 at Carbon Recycling International (CRI) in Iceland. This plant can recycle up to 5500 tonnes of CO_2 into 4000 tonnes of methanol annually. It is situated next to a geothermal energy plant which provides the necessary energy and CO_2 (captured from the power plant's flue gas) for water electrolysis and methanol synthesis (Carbon Recycling International, n.d.). The company also offers a standard plant design for production of up to 100.000 tonnes annually, with one of these currently under construction in Anyang City in China.

Biomass can also be converted to syngas in a gasifier. This syngas contains mostly H_2 and CO, which can then be converted to methanol. For the entire biomass-to-methanol process, Liu et al. (2020) calculated a methanol to material ratio (by weight) of 0.574. This study was based on wheat straw, but this ratio is assumed for the calculations in this research.

2.3. Possible pathways

All possible elements of feedstock collection, treatment and methanol production methods are summarised in a flow chart presented in Figure 2. From this figure, three different pathways are selected that use the various available feedstocks and processes. These will all be explained in the following sub sections, along with calculations of the projected methanol yield based on the available feedstock volumes.

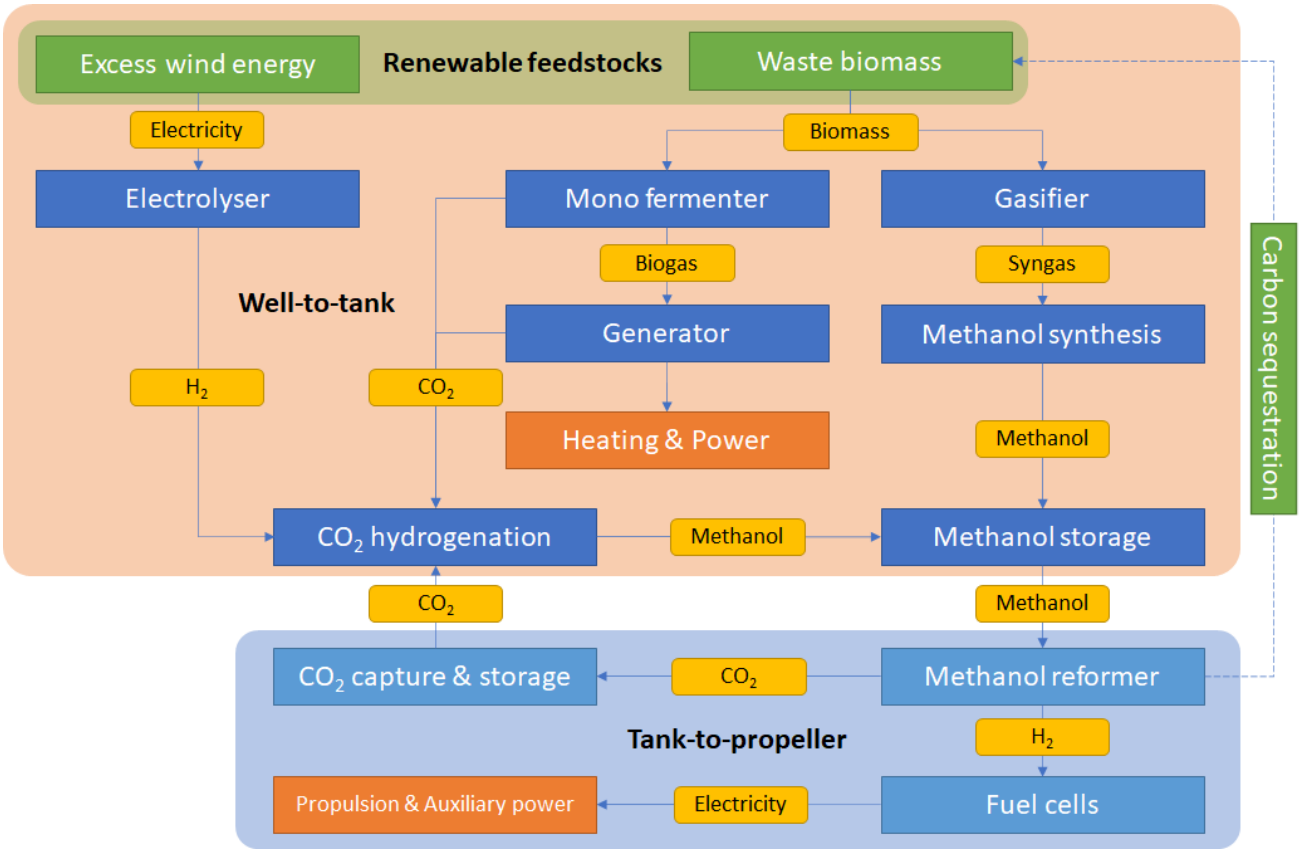

Figure 2: All possible elements that will be considered in order to construct the different pathways.

2.3.1. Bio-methanol via mono-fermentation

This pathway includes methanol synthesised by hydrogenating CO_2, requiring pure H_2 and CO_2 feedstocks. The pathway is visualised in Figure 3. Renewable H_2 will be made from excess wind energy. The CO_2 in this scenario comes from the mono-fermenting process that Rijkswaterstaat will use to produce biogas for the heating and power of its office buildings. A total of 25000 tonnes of (wet) mown grass is used as biomass source, of which 15000 tonnes is collected by Rijkswaterstaat. The mono-fermentation has a pure CO_2 stream as by-product, which is projected to be 3500 tonnes annually. Although not all of this CO_2 stems from Rijkswaterstaat's biomass contribution, it is considered to be available to Rijkswaterstaat if methanol is produced with it. A larger supply of CO_2 is possible if it is captured from the biogas generators that will be used to supply heating and power to RWS offices, but this falls outside the scope of this research.

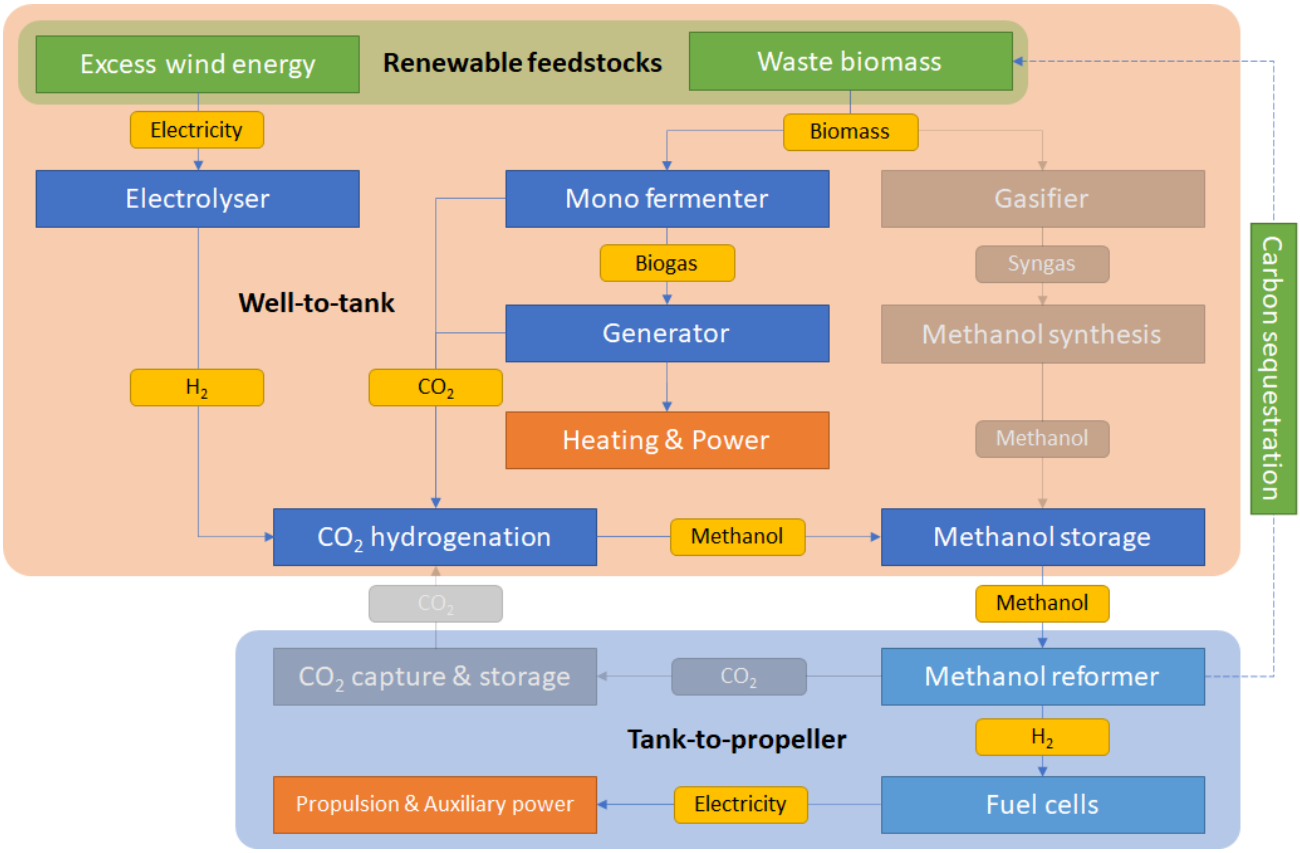

Figure 3: Bio-methanol pathway using CO_2 by-product from mono fermentation of grass biomass, as well as renewably produced hydrogen.

Recalling the main CO_2 hydrogenation reaction:

$$CO_2 + 3H_2 \leftrightarrows CH_3OH + H_2O \tag{2.8}$$

For every mole of methanol, one mole of carbon dioxide and three moles of hydrogen are needed. Therefore, using the molar mass ratios (M) of each substance, the maximum amount of methanol that can be produced is as follows:

$$m_{MeOH,max} = \min\left(\frac{1}{3} \cdot m_{H_2,in} \cdot \frac{M_{CH_3OH}}{M_{H_2}} \; ; \; m_{CO_2,in} \cdot \frac{M_{CH_3OH}}{M_{CO_2}}\right) \tag{2.9}$$

However, losses occur during the process, and not all hydrogen and CO_2 can be converted to methanol. The work of Nieminen et al. (2019) models a standard hydrogenation process, and reports a methanol yield factor of .81, which is defined as the mass (flow) ratio of methanol out and theoretical maximum methanol output:

$$y_{MeOH} = \frac{\dot{m}_{MeOH,out}}{\dot{m}_{MeOH,max}} = \frac{m_{MeOH,out}}{m_{MeOH,max}} = 0.81 \tag{2.10}$$

Assuming a sufficient amount of hydrogen is available and the amount of CO_2 is the limiting factor, 3500 tonnes of CO_2 can be used to produce 2064 tonnes of methanol:

$$m_{MeOH,out} = y_{MeOH} \cdot m_{CO_2,in} \cdot \frac{M_{CH_3OH}}{M_{CO_2}} = 0.81 \cdot 3500 \cdot \frac{32.04}{44.01} = 2064 \text{ [t]} \tag{2.11}$$

Reversing the calculation to obtain the required amount of hydrogen:

$$m_{H_2,in} = 3 \cdot m_{MeOH,out} \cdot {y_{MeOH}}^{-1} \cdot \frac{M_{H_2}}{M_{CH_3OH}} = 3 \cdot 2064 \cdot 0.81^{-1} \cdot \frac{2.02}{32.04} = 482 \text{ [t]} \qquad (2.12)$$

To produce this 482 tonnes of hydrogen, 24 GWh of electricity is needed, well within the 250 GWh available. So indeed, the CO_2 is the limiting factor in this pathway, and it is possible to produce 2064 tonnes of methanol annually. Additional energy is needed for the production process, though most of this can be generated by combusting waste streams. Nieminen et al. (2019) cites a net process electricity consumption of 624 kWh/tonne methanol produced, after combusting these waste streams. This amounts to under 1.3 GWh of electricity used annually, on top of the electricity used for hydrogen production. Since Rijkswaterstaat has plenty of renewable energy available in this scenario, the production of bio-methanol using this process is considered CO_2 neutral.

In the process of hydrogenating CO_2, not all CO_2 and H_2 get converted to methanol. Waste streams contain the excess CO_2 which – unless a carbon capturing installation is added – results in positive CO_2 emissions. The amount of waste CO_2 according to Nieminen et al. (2019) is approximately 14%. In other words, 14% of the carbon dioxide that is obtained from carbon negative sources (biomass) is emitted back into the air during the methanol production process. However, as no additional CO_2 from other non-carbon negative sources is used, the whole system can still be considered carbon neutral, regardless of which part of the systems the emissions occur in. The hydrogen loss as reported by Nieminen et al. (2019) is approximately 17%. A summary of methanol production input, output and emissions is given in Table 1.

	Input	**Output**	**Emissions**
CO_2	3500 t	505 t	505 t
Hydrogen	482 t	80 t	
Methanol		2064 t	
Electricity (hydrogen production)	24 GWh		0 t CO_2eq
Electricity (methanol synthesis)	1.3 GWh		0 t CO_2eq

Table 1: System inputs and outputs for CO_2 hydrogenation based on the work of Nieminen et al. (2019).

2.3.2. Bio-methanol via gasification

If all available grass and woody biomass is used in a gasification process instead of biogas production in a mono fermenter, methanol can be produced directly. The main advantage is that the hydrogen atoms in biomass hydrocarbons are used for methanol, and no external hydrogen supply is necessary. This pathway, visualised in Figure 4, could be attractive if it is decided to fully supply heating and power to the RWS offices with electricity from the grid, while simultaneously supplying green electricity from wind energy to the grid.

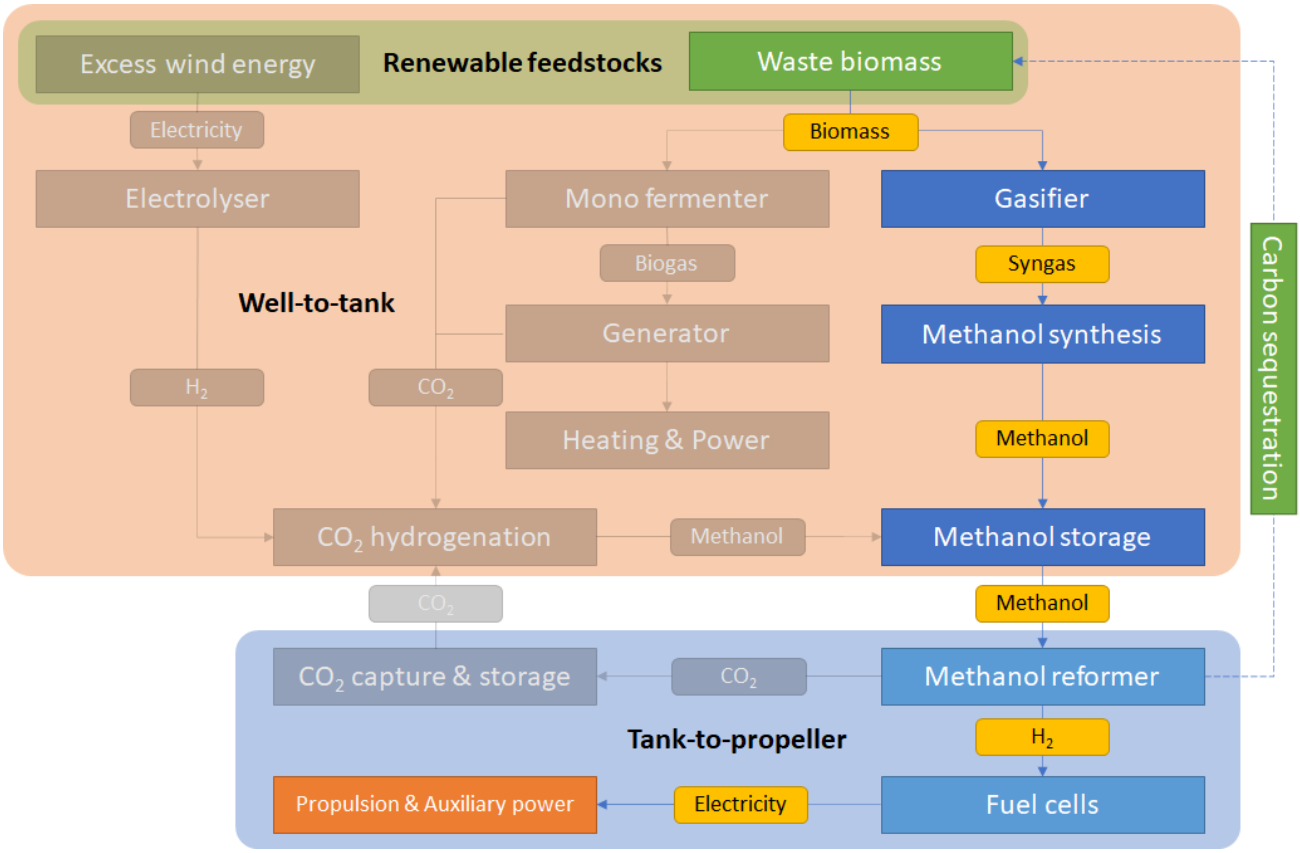

Figure 4: Bio methanol pathway using gasification of biomass.

According to unpublished documents related to the Rijkswaterstaat project to produce biogas from grass biomass, one tonne of wet mown grass results in 0.30 to 0.35 tonnes of dry substance. This is further reduced by 19% to obtain the organic dry substance (ODS) value of 0.243 to 0.284 tonnes ODS per tonne wet grass. Based on these figures, an estimate of 25% wet-to-dry biomass will be used in the further calculations. The annually available grass biomass by Rijkswaterstaat is 15000 tonnes (wet), resulting in 3750 tonnes (dry). With a mass conversion factor of .574 (Liu et al., 2020), this results in 2152 tonnes of methanol.

The process as described by Liu et al. (2020) also produces CH_4, which is collected at the top of the distillation column. Emissions include CO_2, CO and volatile organic substances (VOC). Based on this work, the methanol production input and output are presented in Table 2.

	Input	Output	Emissions
Biomass (wet)	15000 t		
Methanol		2152 t	
CH_4		26 t	
CO_2		0.77 t	0.77 t
CO		1.33 t	1.33 t
VOC		21 t	21 t
Electricity	0.36 GWh		0 t CO_2eq

Table 2: Input and output of the methanol synthesis described by Liu et al. (2020) when using the available grass biomass as feedstock.

2.3.3. Green methanol

Green methanol is produced from renewable, non-biomass sources. For hydrogen, this can again be hydrogen produced in electrolysers powered by excess wind energy. With no non-biomass carbon sources available to Rijkswaterstaat, an alternative solution is found in recycling the carbon compounds of methanol. This can be done by capturing CO_2 from the on-board methanol reformer, storing it on-board and off-loading it to be hydrogenated into methanol again. The same process as biomass-derived CO_2 hydrogenation can be used. As seen in Figure 5, this pathway theoretically results in a completely closed carbon loop (excluding any leakages), not relying on carbon sequestration by plants. However, in practice, CO_2 is emitted during the production of green methanol, as described by Nieminen et al. (2019). It is of course in the best interest of the overall emissions if this can be captured and re-used, but this is outside the scope of this thesis.

The amount of methanol that can be produced this way is limited by the amount of methanol that is used on-board, as virtually all CO_2 can be recycled. An initial supply of (renewable) CO_2 or methanol is necessary, but once all logistics are in place, only an external feed of hydrogen and small external feed of CO_2 (to compensate losses during capture, storage, and handling) is needed. The process is therefore also limited by the hydrogen supply. As mentioned in Section 2.1.1, a supply of just under 5000 tonnes of hydrogen is possible if the entire wind capacity of 250 GWh is used. This would result in an annual methanol production capacity of around 21000 tonnes. However, to further produce methanol using CO_2 hydrogenation, more electricity is needed. Nieminen et al. (2019) reports a consumption of 624 kWh per tonne of methanol produced, which is 2664 kWh per tonne of hydrogen used. Including this additional electricity consumption in the calculation for maximum methanol production, 250 GWh can produce around 20000 tonnes of methanol. Of this 250 GWh, 95% is used for hydrogen production and 5% for methanol production. A summary of the input, output and emissions of methanol production using this pathway is found in Table 3.

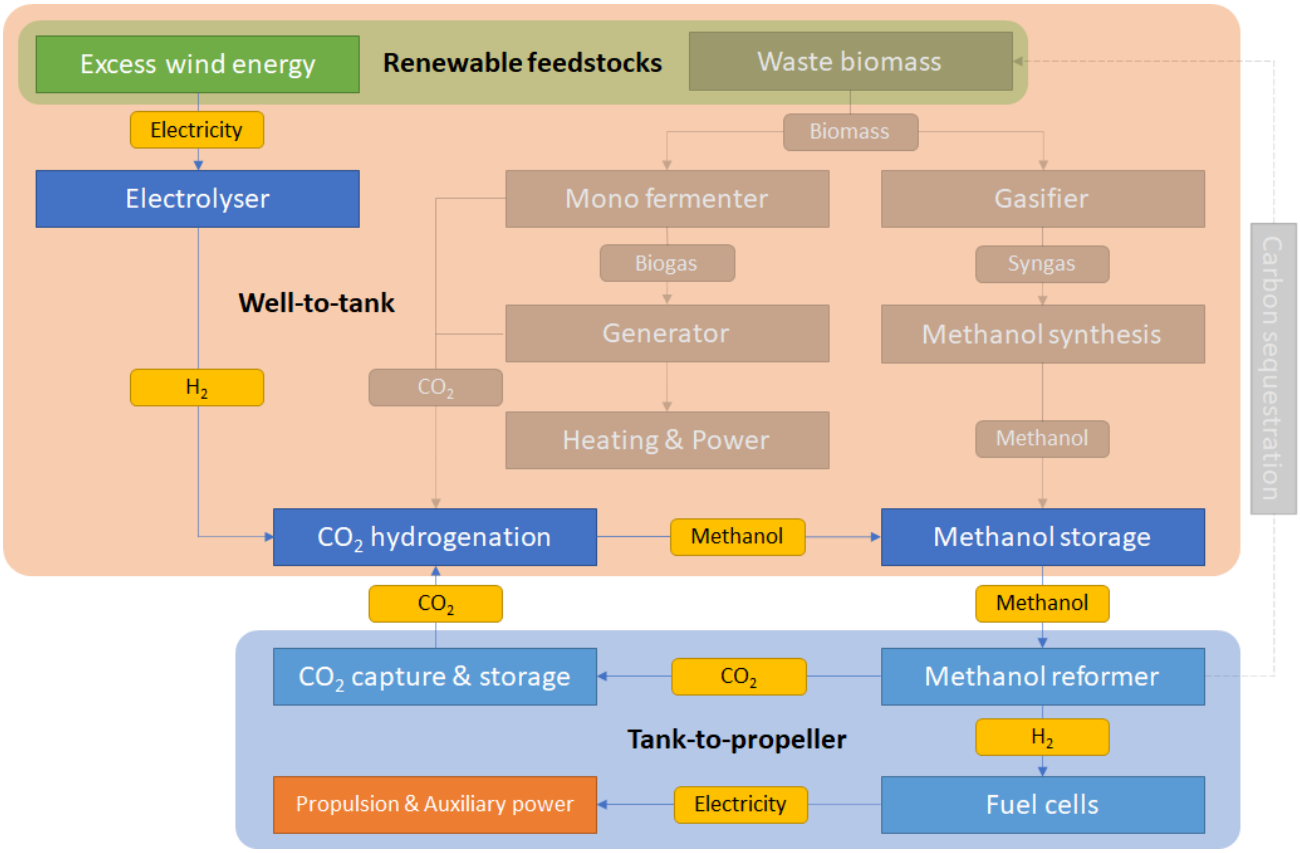

Figure 5: Green methanol pathway using CO_2 hydrogenation using renewably produced hydrogen, and CO_2 from on-board carbon capture.

	Input	Output	Emissions
CO_2	34216 t	4936 t	4936 t
Hydrogen	4711 t	787 t	
Methanol		20177 t	
Electricity (hydrogen production)	237.5 GWh		0 t CO_2eq
Electricity (methanol synthesis)	12.5 GWh		0 t CO_2eq

Table 3: Input/output balance and emissions for green methanol production

2.4. Comparison

Three pathways were identified: bio-methanol via mono-fermentation of biomass, bio-methanol via gasification of biomass and green methanol with on-board CO_2 capture. The first bio-methanol option is dependent on the production of biogas for heating and power of Rijkswaterstaat offices, which is in turn limited by the available amount of grass biomass. Just over 2000 tonnes of methanol can be produced annually. The second bio-methanol option has a similar annual methanol production (2152 tonnes). The green methanol option has the highest possible methanol production: up to 21000 tonnes annually, limited by the available electricity for hydrogen electrolysis. Otherwise, it is limited by the amount of methanol consumed (if all CO_2 emissions are captured on-board): for each tonne of methanol consumed, another tonne can be produced. For a comparison of all required resources and possible methanol production, see Table 4. These pathways can be combined to produce more methanol, which will be discussed in detail in Section 7.2.

	Bio-methanol (1)	**Bio-methanol (2)**	**Green methanol**
Hydrogen feedstock	Wind energy	Gasification of biomass	Wind energy
Electrolyser power consumption	24 GWh		237.5 GWh
H_2 produced/consumed	482 t		4711 t
Carbon feedstock	Mono fermentation of biomass*	Gasification of biomass	On-board CO_2 capture
Biomass consumed	15000 t*	15000 t	
CO_2 consumed	3500 t		34216 t
Production power consumption	0.36 GWh	0 GWh	12.5 GWh
Production CO_2 emissions	505 t	0.77 t	4936 t
Maximum methanol production	2064 t	2152 t	20177 t
Total associated CO_2 emissions	505 t	0 t	4936 t

Table 4: Overview of possible annual methanol production and required resources for the three different pathways. *: biogas is the main product from mono fermenting this biomass feedstock, CO_2 is a by-product.

3. Methanol fuel cells

Fuel cells offer a way to convert chemical energy directly to electrical energy. In contrast to combustion engines, no intermediate heat energy and mechanical energy conversions are required. Engines follow the Carnot cycle principle, which states that there is a maximum of work that can be done in a thermodynamic, the rest is dissipated as waste heat. Fuel cells work on an electrochemical principle, and not on a Carnot limited thermodynamic principle. As such, they can theoretically attain a higher efficiency. However, several other factors limit the efficiency of fuel cells, so in reality they do not always have a higher theoretical maximum efficiency (Dicks & Rand, 2018b). Another advantage of fuel cell systems over combustion engines is the significant decrease in noise and vibrations (Tronstad et al., 2017).

The basic working principle of fuel cells is based on oxidising hydrogen at an anode and a reduction reaction at a cathode. An electrolyte between theses electrodes passes free ions, and an external circuit passes free electrons, inducing a voltage. The exact reactions that take place depend on the type of fuel cell. Most fuel cell systems require hydrogen (at different degrees of purity) as an input to the anode (Dicks & Rand, 2018c). Thus, in methanol powered fuel cell systems, methanol needs to be converted to hydrogen first. This process is called reforming and can be achieved by different processes. After the reforming process, both hydrogen and carbon products (CO_2 and/or CO) are produced. In the context of on-board CO_2 capture this is an important advantage over combustion engines, as a pure CO_2 output is easier to capture than from flue gases that contain various other compounds, which is the case with combustion engines.

The most promising fuel cell types for maritime uses are polymer electrolyte membrane fuel cells (both low and high temperature: LTPEMFCs and HTPEMFCs) and solid oxide fuel cells (SOFCs) (van Biert et al., 2016). Although in a much lower development stage, direct methanol fuel cells (DMFCs) do not require a separate methanol reformer, so they are interesting enough to discuss.

3.1. Methanol reforming

For most methanol powered fuel cell systems, methanol acts as a hydrogen carrier instead of a direct fuel. On-board reformer units should be used to convert methanol to pure hydrogen. The most common reformers use the steam reforming, although other reforming methods are possible too.

3.1.1. Steam reforming

Hydrogen and by-products CO and CO_2 formed from methanol and steam from the following equations (Kundu et al., 2007):

$$CH_3OH + H_2O \leftrightarrows 3H_2 + CO_2 \tag{3.1}$$

$$CH_3OH \leftrightarrows 2H_2 + CO \tag{3.2}$$

$$CO + H_2O \leftrightarrows H_2 + CO_2 \tag{3.3}$$

Equation 3.1 is the so-called steam reforming (SR) reaction, 3.2 the methanol decomposition (MD) reaction and 3.3 the water-gas shift (WGS) reaction. The work of Peppley et al. (1999) showed that all three reactions should be considered when modelling the product gas composition, even though the SR reaction is technically the sum of the MD and WGS reactions. A kinetic model was subsequently constructed in (Peppley et al., 1999a). The works are often cited in literature on this

subject as they explain the full product gas composition, which methods used in earlier works that only considered one or two reactions failed to do (Herdem et al., 2019).

A higher operational temperature increases the hydrogen yield, which can be seen in Figure 6, but it also leads to a higher CO volume fraction. Depending on the type of fuel cell to which the reactant gas is fed, this could lead to poisoning of the fuel cell anode. Therefore, reformer design parameters are different for different types of fuel cells. The CO concentration at different operating temperatures is visualised in Figure 7, where the CO volume percentage is set out against the inverse of the molar flow rate of methanol per weight of catalyst.

Methanol reforming takes place under the influence of a catalyst, which should have a high catalytic activity resulting in high hydrogen production, and an as low as possible CO generation. The most commercially applied catalysts are $Cu/ZnO\text{-}Al_2O_3$ based (Herdem et al., 2019). Research has also been done on other catalysts, including catalysts that have a high activity at lower temperatures. This way, it should be possible to integrate the methanol reformer into the anode of a high temperature PEM fuel cell (Papavasiliou et al., 2012). Direct methanol fuel cells (DMFC) are able to reform methanol directly on the anode, as are solid oxide fuel cells (SOFCs). This will be further discussed in their respective sections.

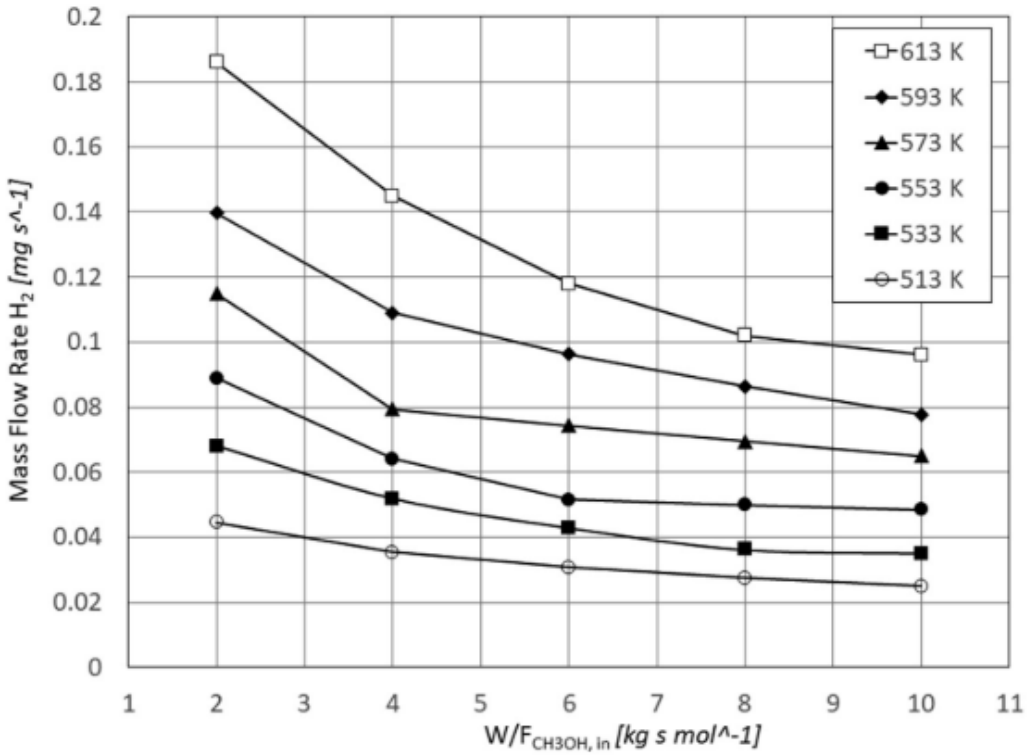

Figure 6: Mass flow rate of hydrogen as a function of catalyst weight / methanol flow rate, for different operating temperatures (Gurau et al., 2020)

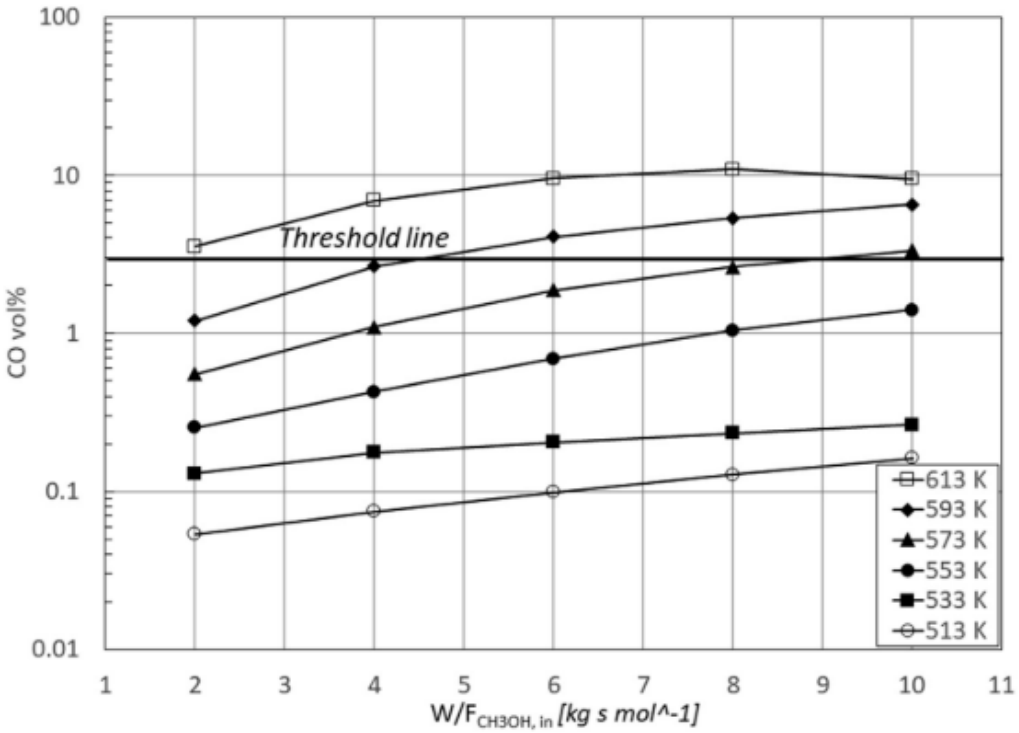

Figure 7: CO volume fraction as a function of catalyst weight / methanol flow rate, for different operating temperatures. The threshold line is based on a 3% CO tolerance of HTPEMFCs (Gurau et al., 2020)

3.1.2. Membrane steam reforming

Membrane steam reforming allows for production and separation of hydrogen in a single stage (Ghasemzadeh et al., 2020). Methanol and steam are pumped continuously through a tubular membrane reactor, where it is converted to hydrogen in the presence of a catalyst. The tube has two streams: the inner permeate stream (containing produced hydrogen) and outer retentate (containing other reaction products and unconverted fuel). The partial pressure difference of the two streams forces hydrogen to pass through the membrane that separates the permeate and retentate (Kim et al., 2019). A sweep gas can be used to remove the hydrogen from the permeate tube, as shown in Figure 8.

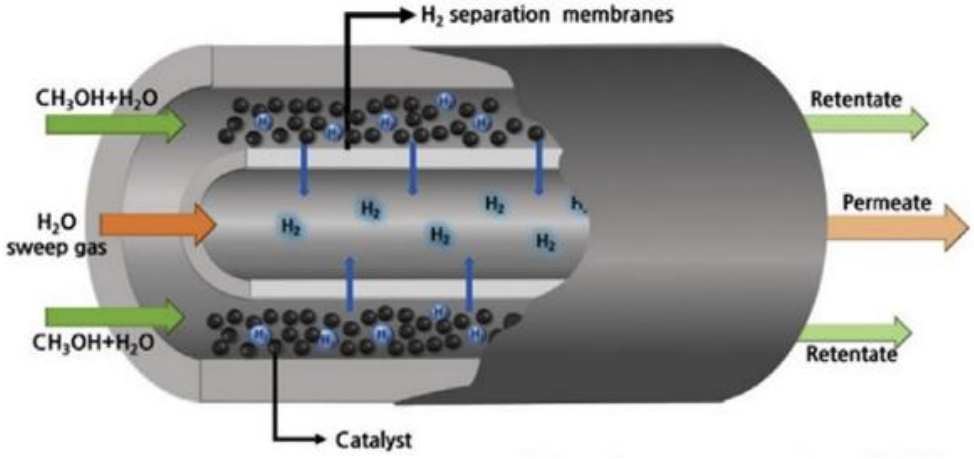

Figure 8: Membrane reactor using steam as a sweep gas in the permeate stream (Kim et al., 2019)

The membrane structure needs to only let hydrogen permeate, which is especially important in low temperature fuel cells that are more susceptible to CO poisoning. Dense palladium membranes are very suitable for this task, but the material is very expensive. Research in various different compound membranes has been done, including both palladium-based and non-palladium-based materials (Lytkina et al., 2019). Some membranes do let other compounds such as CO through, in which case a catalyst is present in the inner tube to promote the water gas shift reaction. A setup like this requires steam to be present in the sweep gas (as seen in Figure 8), in fully hydrogen-selective membranes nitrogen is used (Ghasemzadeh et al., 2020).

3.1.3. Other reforming options

Methanol reforming is not limited to steam reforming. Other options include partial oxidation (POX) and autothermal reforming (ATR).

Partial oxidation suffers from the lowest hydrogen yield (compared to SR and ATR), along with higher emissions of unconverted hydrocarbons and carbon monoxide. Its exothermic process requires high processing temperatures, but it also results in quick dynamic response and start-up. Thermal management is also simpler (Herdem et al., 2019). The low hydrogen yield compared to steam reforming is visible in the POX reaction equation, as only two rather than three moles of hydrogen per mole of methanol are produced (Kundu et al., 2007):

$$CH_3OH + \frac{1}{2}O_2 \leftrightarrows 2H_2 + O_2 \tag{3.4}$$

Autothermal reforming, similar to the autothermal reforming process in methanol production, has the advantage of simplified thermal management, since endothermic and exothermic reactions are balanced such that the process is thermally neutral. ATR systems can therefore also be more compact since fewer heat exchangers are necessary. However, it does complicate control system design to account for thermal balance during load changes and start-up. Further drawbacks are a low hydrogen yield and limited commercial experience (Herdem et al., 2019). Since ATR is a combination of SR and POX, all of the following reactions take place (Kundu et al., 2007), resulting in a hydrogen yield between SR and POX:

$$CH_3OH + \frac{1}{2}O_2 \leftrightarrows 2H_2 + O_2 \tag{3.5}$$

$$CH_3OH + H_2O \leftrightarrows 3H_2 + CO_2 \tag{3.6}$$

$$CO_2 + H_2 \leftrightarrows CO + H_2O \tag{3.7}$$

3.2. PEM fuel cells

Both high and low temperature PEM fuel cells operate on the same principle, where hydrogen oxidised on the anode, releasing H^+ ions and free electrons. A membrane electrolyte passes the H^+ ions to the cathode, where a reduction reaction of oxygen takes place (Dicks & Rand, 2018c). Both of the electrodes (anode and cathode) are usually made of platinum, which catalyses the anodic and cathodic reactions (Valdés-López et al., 2020). The free electrons are passed through an external circuit from cathode to anode, creating an electrical current. The specific reactions for PEM fuel cells are as follows (Dicks & Rand, 2018c):

Anode:	$2H_2 \rightarrow 4H^+ + 4e^-$
Cathode:	$O_2 + 4H^+ + 4e^- \rightarrow 2H_2O$
Total:	$2H_2 + O_2 \rightarrow 2H_2O$

Fuel cells operate at a low voltage, typically around 0.7 Volt. To increase the voltage, multiple individual cells are connected in series to form a fuel cell stack. Between each cell is a bipolar plate, which connects the anode of one cell with the cathode of the next, allowing the electric current to effectively pass through the stack. The anodes and cathodes are respectively fed hydrogen and oxygen by means of separate channels running past the stack and over each anode and cathode. Overall, the system is clamped together to form a sturdy device. Figure 9 shows a stack can be constructed from individual cells with bipolar plates between the cells and end-plates to collect the current, and how hydrogen and oxygen can be fed over the anodes and cathodes. In practice however, the construction of fuel cell stacks is more complicated in order to avoid leakage of gas from the electrolytes, and to allow for the stacks to be cooled with water or air (Dicks & Rand, 2018c).

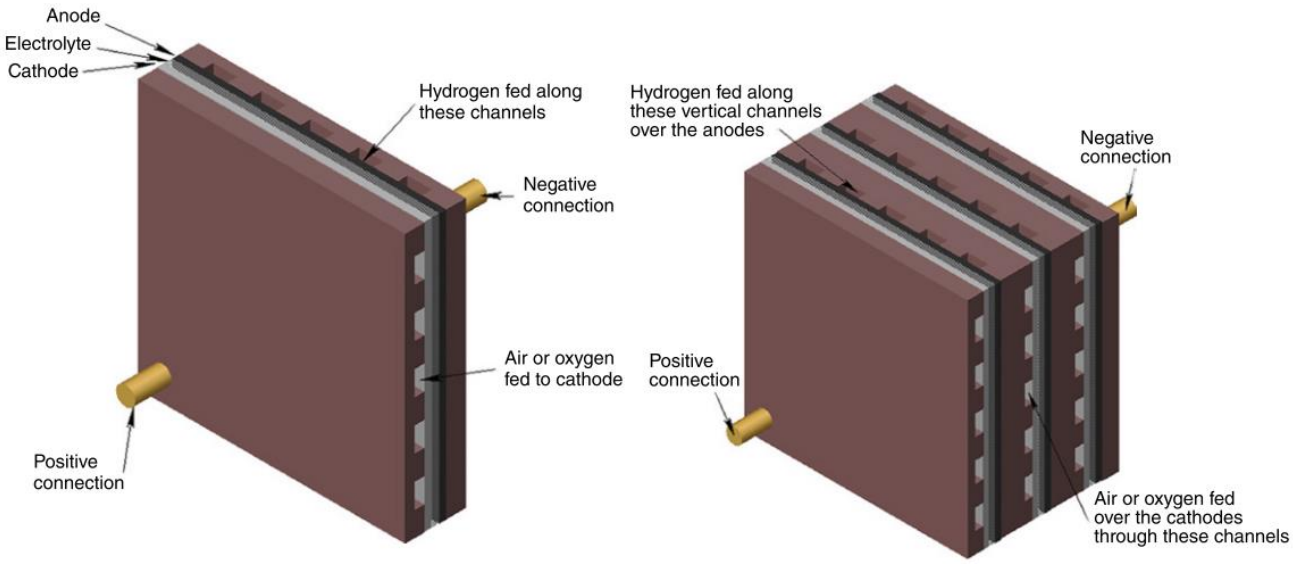

Figure 9: Single cell (left) and three-cell stack (right) connected by bipolar plates, both with end-plates for collecting current (Dicks & Rand, 2018c)

3.2.1. LTPEM

Of all fuel cell types currently on the market, low temperature PEM fuel cells have the highest power density and highest technology maturity in maritime applications (Diesveld et al., 2020). LTPEMFCs use a wetted polymer membrane, which dictates an operational temperature between 65 and 85 degrees Celsius and makes water management more complex (van Biert et al., 2016).

If CO is present in the anode feed gas, it competes with the hydrogen that tries to bond with the platinum anode surface. In fact, CO is more easily adsorbed by the platinum surface than hydrogen. The presence of CO is therefore unfavourable for fuel cell efficiency, as it reduces the rate of hydrogen oxidation on the anode (Valdés-López et al., 2020). This so-called poisoning of fuel cells is inversely dependent on temperature, requiring low temperature fuel cells such as LTPEMFCs to have a higher purity of hydrogen (van Biert et al., 2016).

3.2.2. HTPEM

High temperature PEM fuel cells are a more recent development (van Biert et al., 2016). In order to raise the operational temperature, membranes are used that do not need to be wetted. In fact, liquid water is to be avoided, stipulating a minimum temperature of at least 120°C. The upper temperature limit is usually around 180°C, as higher temperatures accelerate the degradation of the cells (Rosli et al., 2017). A higher operational temperature decreases the susceptibility to CO poisoning, allowing

for less purified hydrogen to be used (Valdés-López et al., 2020). CO concentrations of up to 5% by volume have been reported to be tolerable, for operational temperatures above 180°C (Das et al., 2009). Other works cite a threshold of about 3% (Gurau et al., 2020) However, at these higher CO concentrations both performance and lifetime are impacted (Das et al., 2009).

Another consequence of the higher operational temperature is that it is now possible to use waste heat recovery systems, as the temperature difference with the ambient air is higher. This can improve the overall system efficiency (Rosli et al., 2017). However, overall cell lifetimes for (commercial) high temperature PEMFCs are generally lower than their low temperature counterparts (van Biert et al., 2016).

3.3. SOFC

Solid oxide fuel cells have a much higher operational temperature than PEMFCs, in the range of 600 to 1000 degrees Celsius. These temperatures have several advantages, including cheaper catalyst materials, the ability to reform fuels directly in the fuel cell, and a higher reaction rate. On the other hand, SOFCs require more equipment such as pre-heaters, coolers, heat exchangers and pumps. The fragile ceramic materials that are used in the stack make SOFCs more expensive to manufacture (Dicks & Rand, 2018c). The membrane electrolyte in SOFCs transfers O^{2-} ions from the cathode to the anode. When fuelled with pure hydrogen, the reactions are as follows (Dicks & Rand, 2018d):

Anode: $2H_2 + 2O^{2-} \rightarrow 2H_2O + 4e^-$
Cathode: $O_2 + 4e^- \rightarrow 2O^{2-}$
Total: $2H_2 + O_2 \rightarrow 2H_2O$

In contrast to PEM fuel cells where it is a poison to the anode, CO can act as a fuel at the high temperatures of SOFCs. The following reactions occur (Dicks & Rand, 2018d):

Anode: $2CO + 2O^{2-} \rightarrow 2CO_2 + 4e^-$
Cathode: $O_2 + 4e^- \rightarrow 2O^{2-}$
Total: $2CO + O_2 \rightarrow 2CO_2$

This paves the way for direct internal reforming (DIR) of fuels such as methanol: at the operational temperatures of SOFCs, methanol is heavily favoured to decompose into H_2 and CO (Cimenti & Hill, 2009). Methanol can therefore be directly reformed on the fuel cell anode (Xu et al., 2021), without the need of an external reformer unit. Heat and steam produced by the oxidation of hydrogen can be directly used to reform methanol, which in turn is endothermic and as such reduced the cathode airflow needed to cool the cell (van Biert et al., 2020). This reduces the parasitic power consumption. A schematic overview of a methanol fuelled SOFC with DIR can be found in Figure 10.

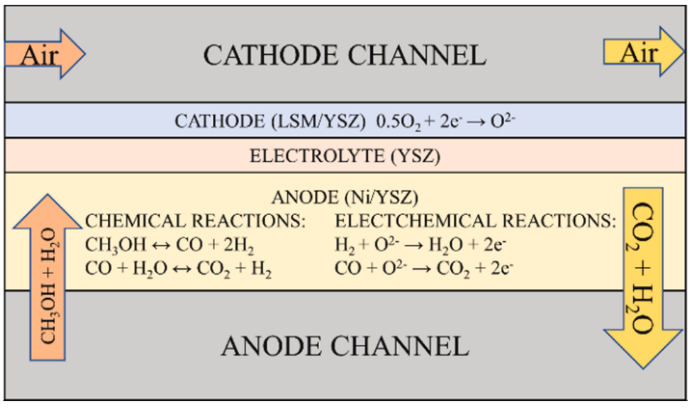

Figure 10: Schematic overview of an SOFC, the anode is supplied a methanol-steam mixture (Xu et al., 2021)

3.4. DMFC

Direct methanol fuel cells are based on PEM fuel cells (Dicks & Rand, 2018a), but do not need a separate reformer unit. Therefore, DMFCs are especially attractive in portable applications such as phone chargers and small fans (Alias et al., 2020). Methanol is oxidised directly on the anode, producing CO_2, H^+ ions and free electrons. Like PEM fuel cells, the H^+ ions and electrons pass from anode to cathode, respectively via the membrane and an external circuit (inducing a current). On the anode, oxygen is reduced to water. The reactions are as follows (Zerbinati, 2002):

Anode:	$\mathrm{CH_3OH + H_2O \rightarrow CO_2 + 6H^+ + 6e^-}$
Cathode:	$\mathrm{\frac{3}{2}O_2 + 6H^+ + 6e^- \rightarrow 3H_2O}$
Total:	$\mathrm{CH_3OH + \frac{3}{2}O_2 \rightarrow CO_2 + 2H_2O}$

A distinction is made between active and passive DMFCs (Burhan et al., 2021). Active systems use components like pumps, valves, and heat exchangers to control the reactant flow, remove waste heat and remove produced water. This water can be recycled to the anode. Passive systems, on the other hand, are much simpler, and do not feature water recirculation. The power densities of passive DMFCs are lower than their active counterparts. In general, the anodic oxidation of methanol in DMFCs is much slower than the oxidation of hydrogen in a similarly sized PEMFC, resulting in a lower power output (Dicks & Rand, 2018a). Along with the low commercialisation level, DMFCs will therefore not be considered in this thesis.

4. Tank-to-propeller model

The second sub question is:

How can the tank-to-propeller greenhouse gas emissions of a methanol fuel cell powered ship be calculated?

In order to answer this question, a MATLAB-Simulink model is constructed that can convert input variables (including operational profile and fuel cell system data) to output variables that can be used to calculate a ship's emissions. The output variables can also be used to determine more specific parameters, such as the installed power and various tank sizes. The model is parametric in the sense that different operational profiles can be loaded so that different ship types can be analysed, as well as providing the ability to change installed systems (such as fuel cell and reformer systems).

4.1. Input data

The general model structure is as follows: MATLAB is used to import input data (from both Excel files and MATLAB scripts) and change parameters. The main script provides the ability to change to different ships and fuel cell systems. The model itself is built in a Simulink environment, which produces several output vectors and values. The model itself can be seen in Figure 11, from which several sub models will be explained further in this Chapter. Graphical interpretations are made using MATLAB again. Most of the analyses require the model to be run multiple times (for example changing the number of installed systems), which is handled inside the MATLAB scripts as well.

4.1.1. Operational profile

The operational profile data is structured as in Figure 12, which shows the data for the ETV. An explanation for each column is given below:

- Ship: lists the ship type
- Task: main task name, multiple lines can be used for each main task
- Task%: the percentage of operational time that is spent performing each main task
- t_year: the yearly operational time spent performing each subtask
- Subtask: subtask name, can be one or multiple for each main task
- Subtask%: time spent performing each subtask, as a percentage of the main task
- Autonomy: minimum time that the ship should be able to perform this task per trip
- P_max: maximum (shaft) power demand
- P_max%: percentage of sub task time sailing at maximum power
- P_max_h: hours per sub task sailing at maximum power
- P_avg: average (shaft) power demand
- P_avg%: percentage of sub task time sailing at P_a
- P_avg_h: hours per sub task sailing at P_avg

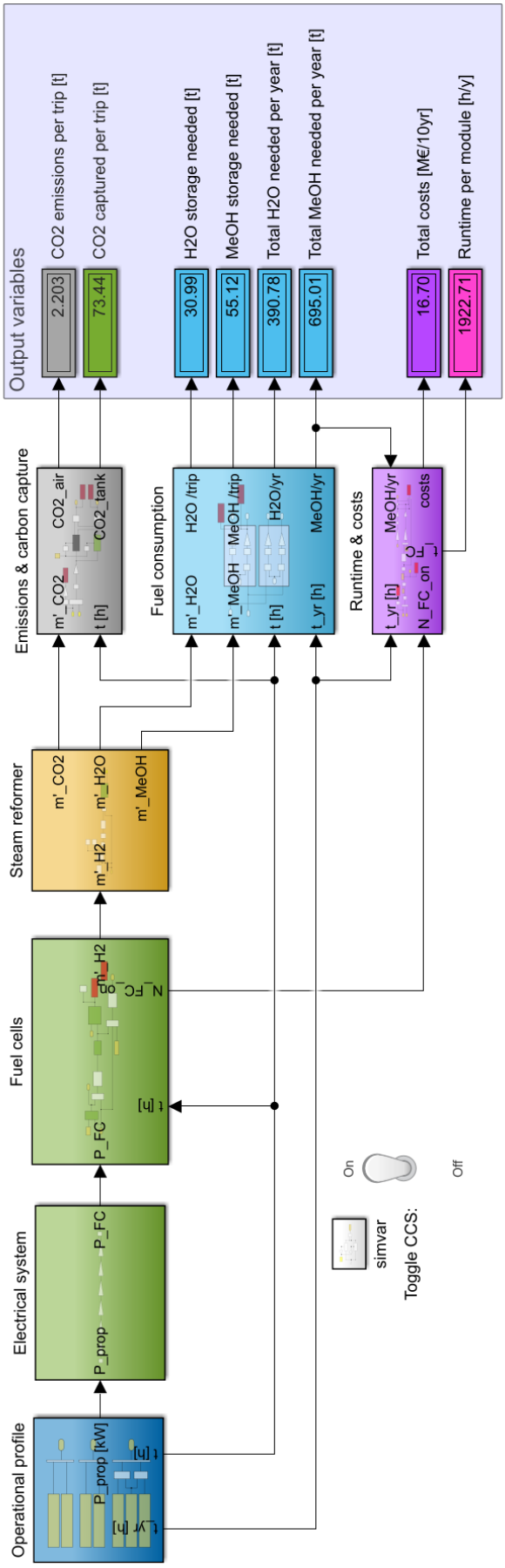

Figure 11: Main Simulink model

Ship	Task	Task%	t_year	Subtask	Subtask%	Autonomy	P_max	P_max%	P_max_h	P_avg	P_avg%	P_avg_h
ETV	Towing	1.2%	10 hrs	Mobilisation	10%	5 hrs	6000 kW	20%	1 hrs	1500 kW	80%	4 hrs
ETV	Towing	1.2%	93 hrs	Towing	90%	43 hrs	8000 kW	30%	13 hrs	5500 kW	70%	30 hrs
ETV	Stand-by	98.8%	2116 hrs	Mobilisation	25%	84 hrs	4000 kW	20%	17 hrs	2000 kW	80%	67 hrs
ETV	Stand-by	98.8%	6349 hrs	Towing	75%	252 hrs	500 kW	20%	50 hrs	250 kW	80%	202 hrs

Figure 12: ETV operational profile input table.

The model can handle power demand of zero, for example for ships that use shore power during some of their operational time. The Simulink model uses the maximum and average power levels (P_max and P_avg) along with the respective durations (P_max_h and P_avg_h) for the calculations for each trip. This is done by constructing a power vector containing all different power levels, and a corresponding time vector containing the durations. A similar vector is constructed for the yearly total time spent at each power level. The way this is done in Simulink is shown in Figure 13.

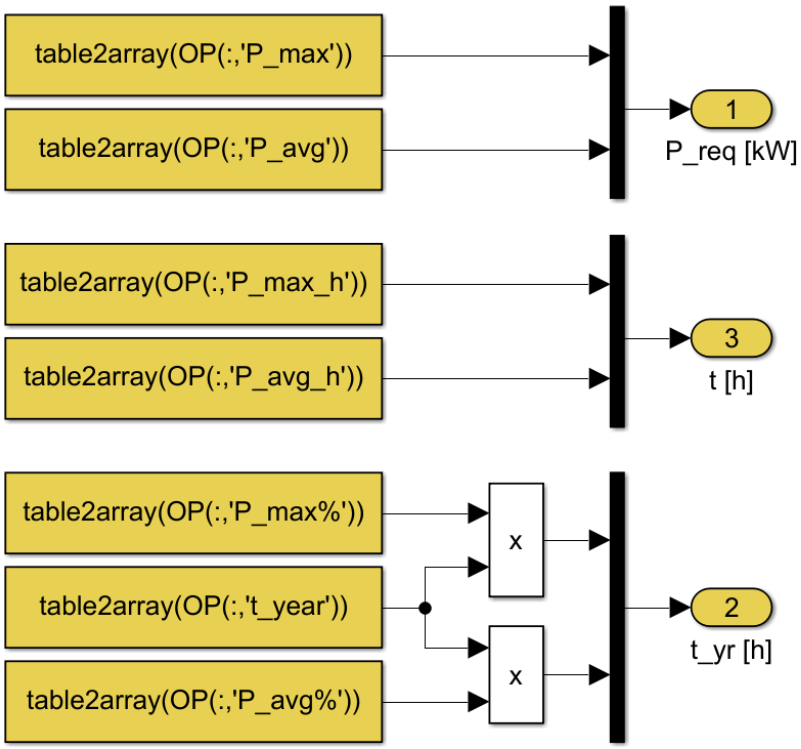

Figure 13: Operational profile subsystem, showing how the power vectors and time vector are constructed.

4.1.2. Fuel cell and reformer data

The fuel cell data is, like the operational profile data, derived from an Excel input file. This excel file can contain multiple named sheets with different fuel cell systems, which can be switched to in the main model file. This way, different fuel cell systems can be used when running the model. The most important fuel cell data are the power output and efficiency, from which the fuel consumption can be calculated using the lower heating value (LHV) of hydrogen:

$$\dot{m}_{H_2} = \frac{P_{req} \cdot \eta_{FC}}{LHV_{H_2}} = \frac{[\mathrm{kW}] \cdot [-]}{[\mathrm{kWh/kg}]} = [\mathrm{kg/h}] \tag{4.1}$$

An example efficiency and fuel consumption diagram can be found in Figure 14, which uses data based on the PowerCellution MS200 LTPEM fuel cell system.

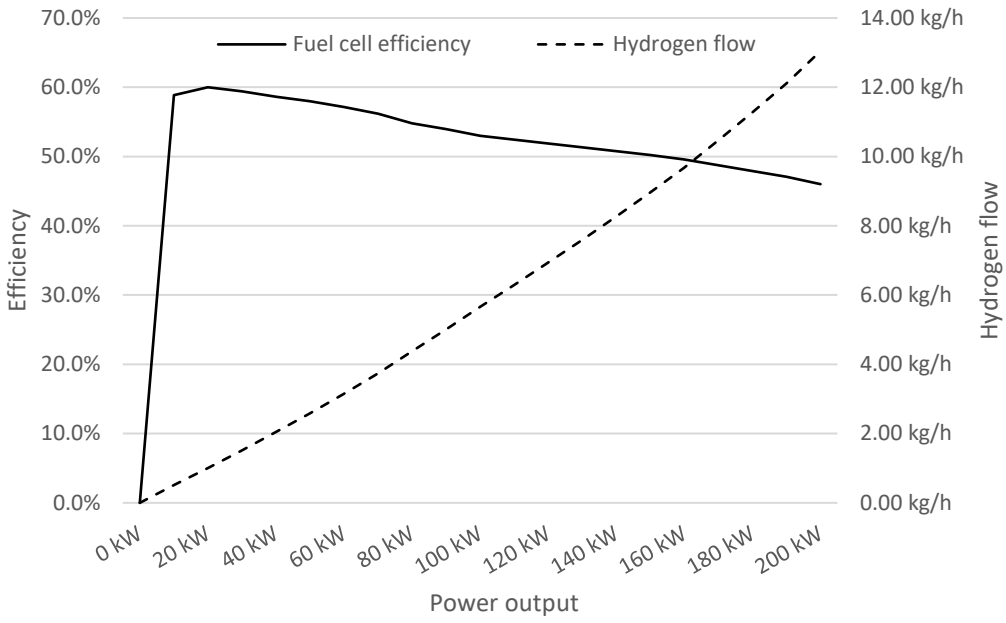

Figure 14: Fuel cell efficiency and hydrogen fuel flow curve of the MS200 LTPEM system.

4.2. Electrical system

The power demand as described by the operational profile is the propeller power demand. To calculate the required power output of the fuel cell systems, efficiencies of several power conversion steps are required. Between the fuel cells and the propeller, the following systems are present:

- DC/DC converter
- DC/AC converter, to convert DC power into AC power
- AC switchboard
- AC/AC frequency converter
- AC electric motor, to convert electrical power into mechanical power
- Gearbox, to change the rotational speed of the shaft line

As different ships can have other electrical system lay-outs with different efficiencies, the exact values for each efficiency are variable parameters which can be changed in the operational profile input (Excel) file. If any default components are not present, they can be omitted by using “1” as efficiency, and extra components can be added using the “Extra efficiency” value. For the ship types reviewed in this thesis, an overview of the electrical system can be found in Figure 15. In these cases, the total power demand from the fuel cell systems is calculated as follows:

$$P_{FC} = \frac{P_{prop}}{\eta_{DC/DC} \cdot \eta_{DC/AC} \cdot \eta_{AC/AC} \cdot \eta_{emAC} \cdot \eta_{GB}} \tag{4.2}$$

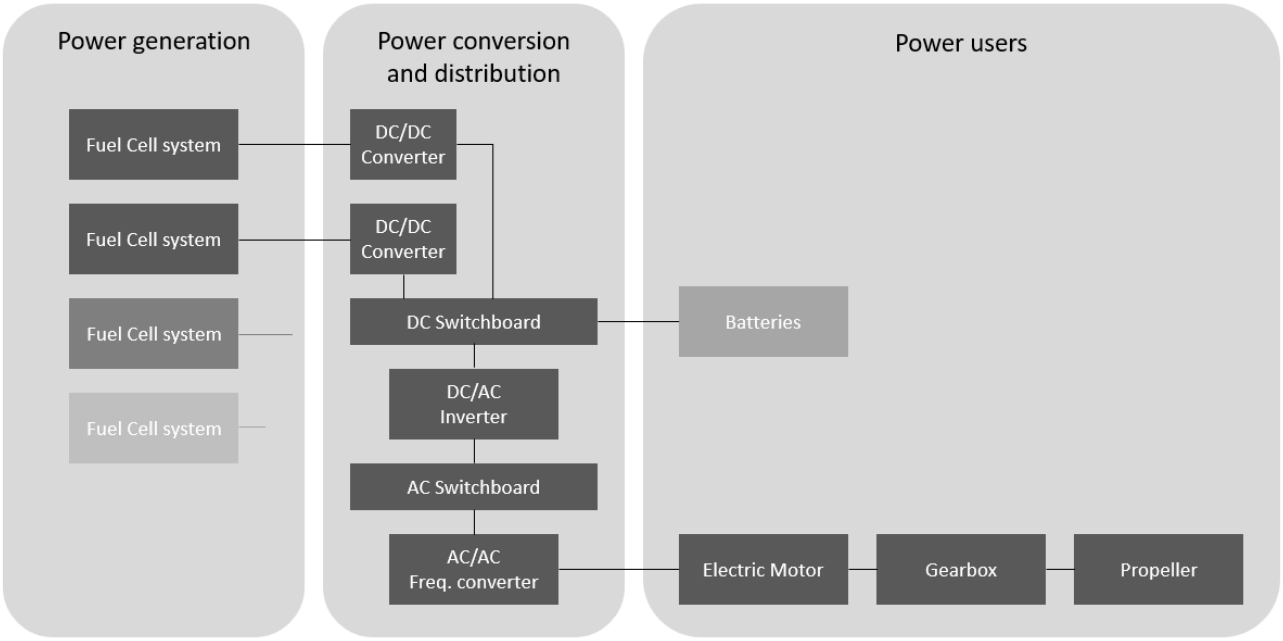

Figure 15: Electrical system overview for the reviewed ship types. Batteries are not included in the model.

4.3. Fuel cell systems

The fuel cell sub model converts the power demand to a hydrogen demand. Since fuel cells have their most efficient working point at a low power output, it is interesting to look at the number of systems that are operational at the same time. Whenever all systems are operational at the same time (at maximum power demand), the overall efficiency is lowest. But at half power for example, either all systems can operate at half power, or half of the systems can operate at full power. The former situation provides a higher overall efficiency. As the lifetime of fuel cell stacks is a finite number of operational hours, the latter situation results in a longer overall fuel cell lifetime, in turn resulting in longer periods between investing in fuel cell systems. This balance between lifetime and efficiency is managed by changing the number of simultaneously online systems. For each power level, a minimum and maximum number of systems are determined, based on the power output of each system and the total installed power. By default, the model uses the average of these values. An overall model parameter modifies this number, so that the model can be run with different numbers of online systems, resulting at different efficiency levels. For example, the relationship between fuel cell efficiency and total operational fuel cell time can be visualised, as seen in Figure 16. Here, the above statements are confirmed: a higher efficiency also uses more fuel cell hours per trip and result in a shorter lifetime.

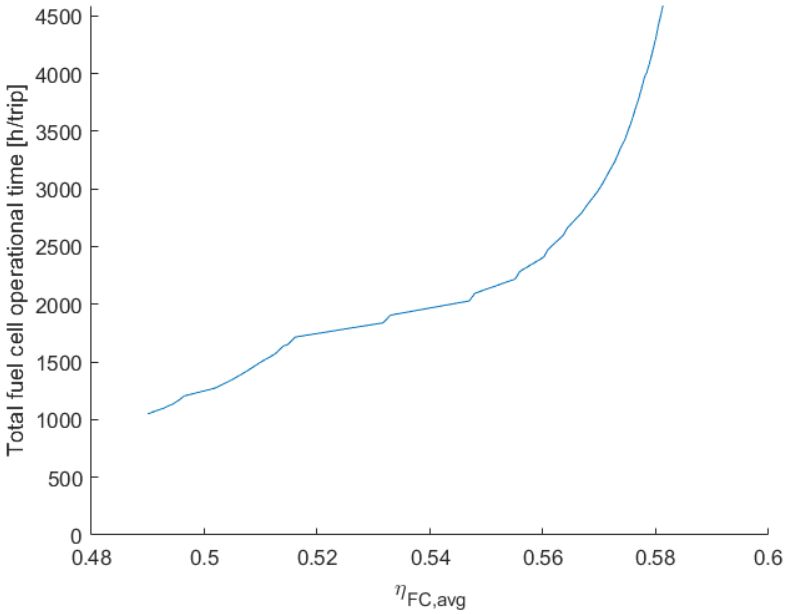

Figure 16: Total operational fuel cell hours compared to fuel cell efficiency.

4.4. Runtime and costs

In order to determine the optimal number of installed fuel cell systems and the corresponding optimal efficiency (based on the number of systems online at the same time), two main cost indicators are considered. The methanol costs are based on the annual fuel consumption (as described in Section 4.6) and a fixed price of €800 per tonne. The costs of fuel cell systems are expected to decrease as production ramps up (Kleen & Padgett, 2021), so it is interesting to see if investing in more systems upfront (prolonging the lifetime and thus time between investments) outweighs the effect of this price decrease. The price point used in this analysis is €2500 per kW, decreasing to €1000 per kW within 30 years. All price points and development of the fuel cell price are configurable. In this analysis, both the fuel cell price point over time and efficiency play a part, so this can contribute to the balance between using a higher efficiency or improving lifetime.

Figure 17 shows an analysis of the relationship between installed power on the total costs. This analysis is of course price dependant, but it does show several interesting trends. Firstly, for higher amounts of installed power, the average efficiency goes down. This is due to the model “choosing” the most cost effective operational parameter (number of simultaneously online systems). In other words, it shows that if enough power is available, it is better to increase the system’s lifetime than it is to increase the efficiency. This balance could fall the other way if fuel cell costs are significantly decreased compared to methanol costs. Another interesting trend is the total costs that increase with installed power. This is mainly due to the assumed rate at which investment costs decrease: in this scenario it is more cost efficient to only pay for the minimum required amount of systems and replace them earlier. If the fuel cell prices would not decrease at all, this would have the opposite trend: the investment costs over time would be the same, so it is more cost effective to have more systems available to decrease the operational hours and prolong lifetime. However, this analysis does not include the added space that is needed on board.

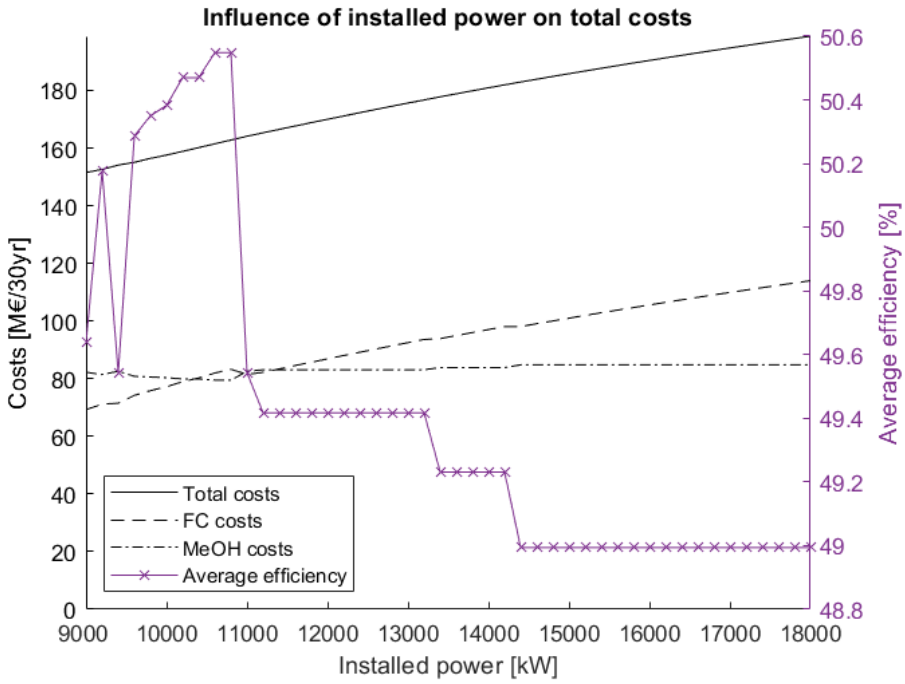

Figure 17: Influence of the total installed power on the fuel cell costs, methanol costs and total costs over 30 years.

4.5. Reformer systems

The number of reformer systems that are online is dependent on the fuel cell hydrogen demand. As the model uses data from reformer systems that are assumed to have a constant efficiency, the number of online reformer systems is simply the hydrogen demand divided by the maximum hydrogen production of each system. In other words, hydrogen is produced by as few simultaneously online systems as possible, working near maximum capacity. This reduces the number of overall operational hours and is thus expected to reduce maintenance and/or replacements costs. If reformer systems with a non-constant efficiency curve are used as input, the model can be changed to incorporate the balance between efficiency and lifetime in the same way as in the fuel cell sub model.

Based on the hydrogen demand, the reformer sub model calculates the amount of methanol and water that are needed for hydrogen production, as well as the CO_2 that is produced in the process. Recalling the main steam reforming reaction:

$$CH_3OH + H_2O \leftrightarrows 3H_2 + CO_2 \tag{4.3}$$

For each three moles of hydrogen, one mole of methanol and one mole of water are needed, producing one mole of carbon dioxide. First, the hydrogen demand is divided by the reformer efficiency, which is expressed as the ratio between the actual and theoretical maximum hydrogen output. Then, it is divided by the molar mass to obtain the molar flow, which can be used to obtain the molar flow (and subsequently the mass flow) of the other reaction components, as shown in Figure 18.

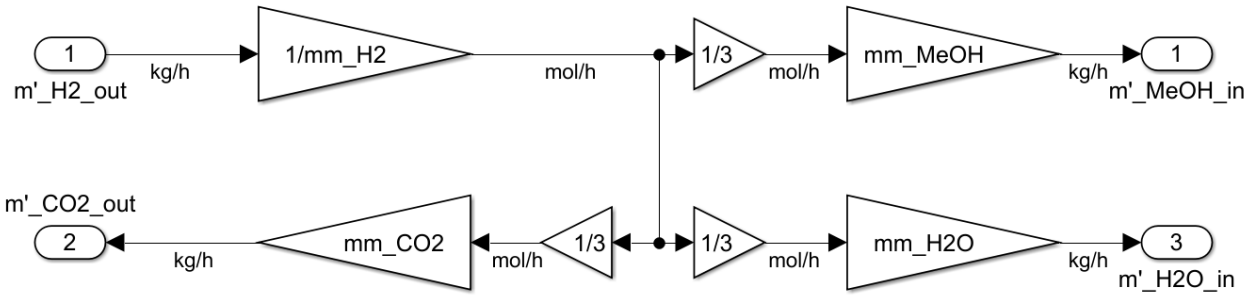

Figure 18: Reformer reaction kinetics sub model

4.6. Fuel consumption

The amount of methanol consumed is derived from the reformer sub model output. The methanol flow is converted to a methanol demand by multiplying the flow vector with the time vectors from Section 4.1.1. This results in both a methanol consumption per trip (when multiplied by the trip time vector) and per year (using the yearly time vector). The same is done for water consumption, as deionised water needs to be stored on board in order to generate steam for the steam reforming reaction.

4.7. Emissions and carbon capture

The carbon dioxide flow output from the reformer section is handled in such a way that it incorporates the ability to store CO_2 on board. Other inputs are the trip time vector, CO_2 storage tank size and capture ratio (percentage of CO_2 that can be captured). For every trip, the total amount of produced CO_2 is calculated by multiplying the flow and time vectors and summing the elements of the resulting mass vector. Part of this CO_2 is always emitted into the air, the other part is stored on board, if enough capacity is available. If tank limits are reached, the remaining CO_2 will all be emitted. The outputs of this sub model are therefore the CO_2 emissions per trip and the amount of CO_2 captured and stored per trip. This data can then be further handled to calculate the yearly emissions. For an example where an analysis is done on the yearly emissions depending on storage tank size, see Section 6.3.1.

4.8. Model limitations

The tank-to-propeller model is limited in a few ways. First of all, since it is not a dynamic model, dynamic load changes and their impact on fuel cell lifetime are not taken into account. Batteries can be used to limit the rate of load changes on fuel cells, limiting the lifetime impact, but this is also not included in the model. It is therefore unknown how large battery systems are needed for this purpose. Lastly, some of the scripts used for analyses are ship-specific. One example of this is the ETV, where sometimes the “normal” operational profile should be used for analysis, and sometimes the operational profile that includes emergency towing. Therefore, the model is not 100% parametric as some scripts need modification before being able to be fully compatible with other ship’s input files, but it does work without major modifications for ships with operational parameters comparable to the three case studies.

5. On-board integration

The third sub question is:

How can methanol fuel cells and a carbon capture system be integrated into a Rijksrederij ship?

This Chapter will discuss the technical implementation of methanol fuel, reformers and fuel cells on board of a ship. First, a selection of ships is made that will be analysed in detail. The current components and system layout will be reviewed, and subsequently the amount of space that can be made available for methanol fuel cell systems. The possibility of integrating carbon capture and storage systems is also investigated. Some system parameters follow from the operational profiles, others (such as methanol consumption and CO_2 output) are iterated from the previous Chapter, where a model was constructed to calculate the tank-to-propeller emissions, but which also gave the ability to determine various system parameters.

5.1. Ship selection

The selection of ships that will be considered more in-depth is made based on different criteria. First, the greatest benefit in emission reduction is made if the vessels that currently emit the most greenhouse gases are converted to operate carbon neutral. Secondly, vessels that are set to be replaced or refitted in the coming years will be considered. As a large part of the Rijksrederij fleet is set to be replaced or refitted in the coming years, but not all vessels can be considered in detail. Previous research by the Rijksrederij has identified a part of the fleet that is fit to use methanol, listed in Table 5. It includes emergency towing vessels, multi purpose vessels and smaller patrol vessels. It is therefore useful to select representative ships for each of these categories to analyse in more detail, from which conclusions can be extended to other vessels in Chapter 7.

Vessel	No. of vessels	Length	Displacement	Installed power
ETV	3	66 m	4000 t	8900 kW
MPV-50	4	50 - 60 m	1200 t	2200 kW
RWS70	10	24 m	67 t	1000 kW
MPV-200	2	60 m	2000 t	3500 kW
MPV-100	1	75 m	3000 t	2500 kW
MPV-50 A1	1	75 m	3500 t	3000 kW
Patrol vessel 1B	3	15 m	20 t	1000 kW
Patrol vessel 2B	11	18 m	25 t	1000 kW
Patrol vessel 3B	7	22 m	35 t	1500 kW
RHIB	6	10 m	3 t	300 kW

Table 5: List of Rijksrederij vessels identified to sail on methanol by 2030.

5.1.1. Highest possible emission reduction

The majority of the Rijksrederij emissions currently stem from the large sea-going Emergency Towing Vessel (ETV) Guardian. With two more ETVs entering into service within the next year, more than half of the Rijksrederij's emissions are expected to stem from these vessels. Therefore, focussing on making these vessels sail carbon neutrally could make the greatest impact on overall emission reduction. As most info is available on the ETV Guardian, this vessel is used as the basis for all calculations and analyses.

The ETVs are not owned by the Rijksrederij but rented from third parties. Therefore, converting these vessels is a challenge management and policy wise. However, this fact does not change the technical analysis in this thesis.

5.1.2. Newbuilds

A range of multi purpose vessels (MPVs) is in the process of being designed and commissioned by the Rijksrederij. This vessel type is called MPV-50 and is set to replace a range of different, older vessels. The MPVs will be equipped for various different tasks, including buoy handling and maintenance, measuring tasks, patrolling and responding to incidents. As no current design is available, an older design will be used as the basis for integration of components.

5.1.3. Refits

A series of fast patrol vessels (RWS 70 series) is subject to be refitted within the next few years. This series consists of eleven vessels, currently sailing on diesel engines.

Of the three vessel types identified in this section, the RWS70 is the most interesting space-wise. It has a small engine room with no space to expand, and its fuel tanks are located at the sides of the vessel. As regulations usually dictate fixed safety margins (in regard to for example cofferdams surrounding fuel tanks), smaller vessels require relatively more extra room for these features compared to larger vessels.

5.2. Current situation

Before looking into fitting the required systems on board of the selected ship types, the current situation is evaluated. Since the prime movers, fuel tanks and related equipment are all to be replaced, these are "removed" from the ship so that the available space for new systems can be determined.

5.2.1. ETV Guardian

The ETV Guardian is powered by two 4000 kW diesel engines (MAK 8M32C), each directly driving a controllable pitch propeller. Two Volvo Penta 410 kW generators provide auxiliary power, with a 100 kW backup generator. Three 600 kW tunnel thrusters are installed: two at the bow and one at the stern.

The current fuel tank layout of the ETV Guardian is seen in Figure 19. In total, the vessel can carry 540 tonnes of HFO (535 m^3) and 305 tonnes of MGO (355 m^3). The HFO tanks can also be used for MGO, which is how the Rijksrederij currently uses these. Since the vessel has firefighting capabilities, firefighting foam is also stored in tanks. Other tanks include ballast and freshwater tanks as well as tanks for recovered oil.

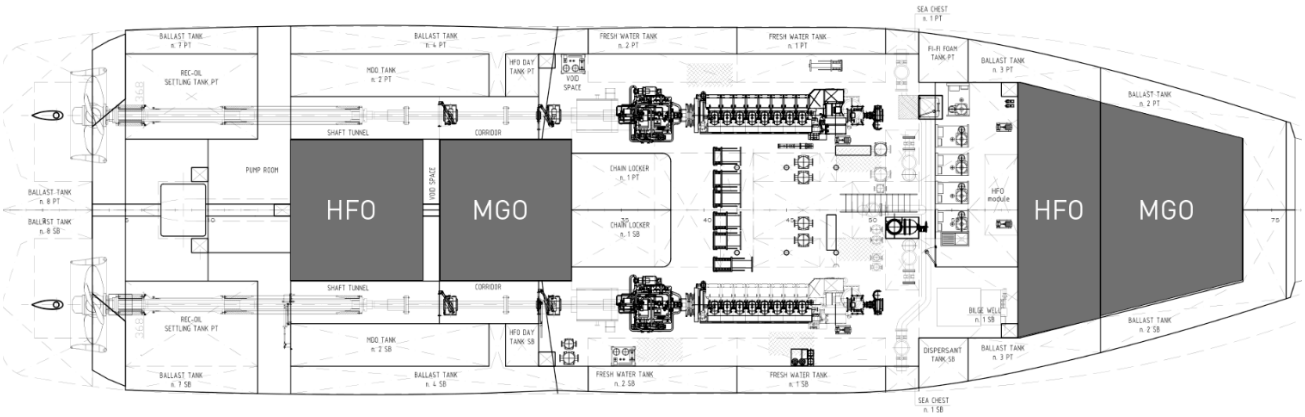

Figure 19: Current fuel tank locations on board of the ETV Guardian.

When all existing machinery is removed from the ship, two empty decks of around 365 m^2 and one room of around 46 m^2 are left, along with some other empty spaces. This is the full footprint that can be used for fuel tanks, reformer systems, fuel cell systems, carbon capture and storage systems, as well as all related safety and auxiliary equipment.

5.2.2. RWS70

The RWS70 has two 651 kW Caterpillar C18 main engines and a 99 kW Caterpillar C4.4 generator. Each main engines directly drives a propeller. Two 3.25 m^3 MGO tanks are located at the sides of the vessel. The current engine room layout of the RWS70 can be found in Figure 20.

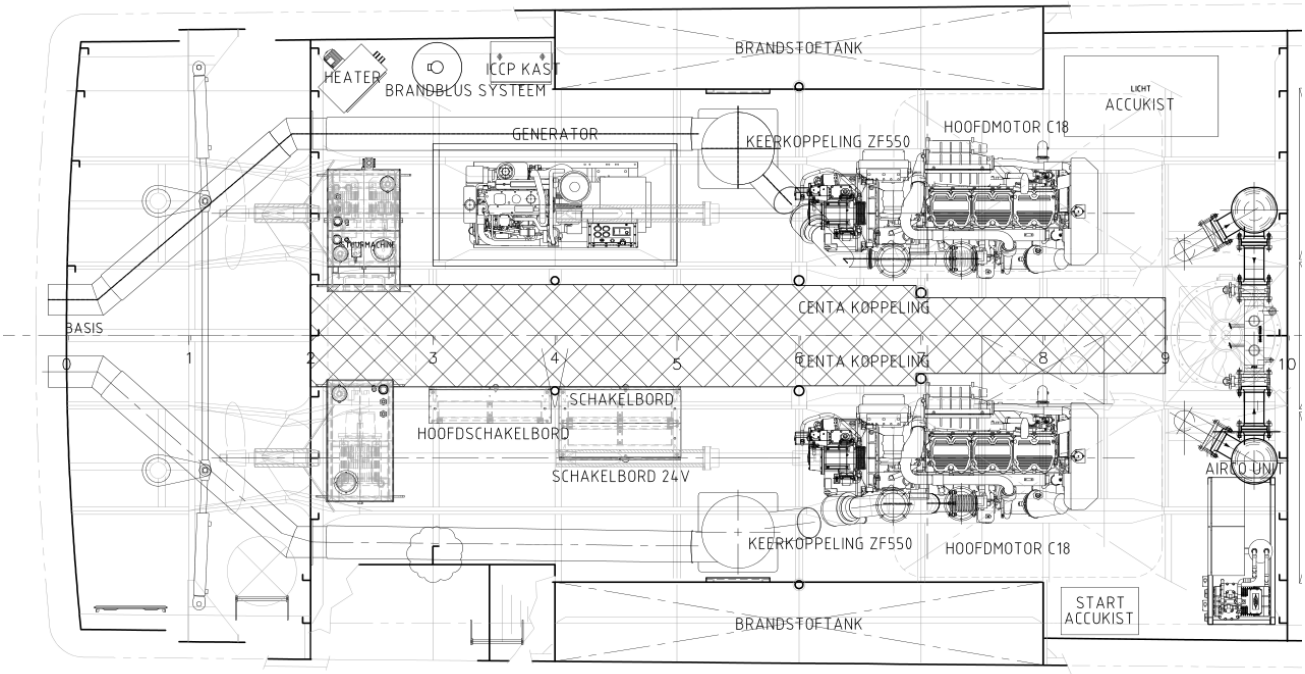

Figure 20: Engine room layout of the RWS70.

5.2.3. MPV

The MPV is based off a confidential design. Therefore, no general arrangements or statements about the current situation will be present in the main thesis, although drawings will be available in a confidential appendix. Henceforth, only general statements about requirements will be made.

5.3. Fuel cell systems

Two important factors are considered when on board fuel cell systems are considered: fuel cell type and regulatory limitations. The former impacts the design mostly in terms of choice of other systems (including reformers) and floor space usage, the latter dictate requirements for all types of fuel cell systems, regardless of the type chosen.

5.3.1. Choice of fuel cell type

The different suitable fuel cell types were previously discussed in Chapter 3. For the different ship types, different fuel cell types are preferrable. As this thesis is partially based on using products that are commercially available, a list of known fuel cell manufacturers was constructed, sorted by type of fuel cell. All known relevant parameters (size, mass, power output, fuel usage, efficiency, lifetime) were compared, as far as possible.

The choice between LTPEM, HTPEM and SOFCs (DMFCs were already discussed to be not considered in this thesis, see Section 3.4) was first made based on commercial availability. It is in the interest of the Rijksrederij to focus on systems that are commercially attractive. As no full commercial SOFC systems were found, the focus went to both PEM options. The most interesting commercially available HTPEM system suitable for maritime usage is the Serenergy HT5000, which is a small 5 kW system with built-in reformer. However, the limited power density makes it less suitable for space restricted areas such as ships. Multiple HT5000 units can be stacked in a rack, but this still requires a large footprint area, at 15 kW/m^2. LTPEM systems have the advantage of having higher power densities, a longer lifetime and higher commercialisation level. Of all systems that were found, the PowerCellution Marine System 200 (MS200) is the most energy dense system, while also having a high maximum efficiency (up to 60%). The power-to-footprint ratio is 317 kW/m^2, more than 20 times higher than the previously mentioned HTPEM systems. However, the HT5000 systems include reformer systems, while the MS200 needs separate reformers. Including the footprint of the Element 1 M13 reformers (of which two are needed per MS200), the MS200-M13 combination is still preferable over the HT5000, as its combined power-to-footprint ratio is still twice as high. The decoupling of reformer and fuel cell systems further allows for carbon capture systems to be used between the reforming of methanol to hydrogen and CO_2, and the fuel cell stack itself. For these reasons this is the type of fuel cell that is used in the further analyses.

5.3.2. Regulatory limitations

According to class rules, fuel cell spaces must be gas tight and separate from accommodation and other machinery spaces (DNV GL, 2020). It is preferred to have a direct access point from the open deck, or else an airlock should be installed. Fuel cell spaces may contain methanol reformers, as long as the fuel cell space is also compliant to rules regarding handling methanol inside. As hydrogen is a light and volatile gas, the ceiling of fuel cell spaces must be geometrically shaped such that any leakage freely flows to ventilation outlets. This ventilation system must only serve the fuel cell room, and be equipped with two separate fans, each being able to ventilate 100% of the room. Fuel cell spaces are regarded as machinery spaces of category A (following SOLAS CH.II-2). Notable extra requirements regarding fire safety are A60 insulation to all surrounding spaces and fixed fire-extinguishing systems suitable for hydrogen technology. All hydrogen piping should be double-walled, with the outer walls being able to contain any leakages. One solution is to fill the secondary enclosure with nitrogen whilst monitoring the pressure. Another acceptable solution is to use fully welded pipes, as long as the fuel cell space ventilation can dilute gas concentration sufficiently to avoid it being in the flammable range.

5.3.3. Installed power

As concluded from the tank-to-propeller model in Section 4.4, it is not more cost-efficient to install more power than necessary for the operational profile. Therefore, the three vessels will be equipped with enough power to reach their maximum power demand, which for the ETV and RWS70 is based on the current installed power. The maximum power is respectively 8000, 1000 and 2200 kW for the ETV, RWS70 and MPV. By changing the drive system to an electrical instead of a mechanical drive, some power is lost in electrical conversions (see Section 4.2). Therefore, the actual installed power (measured at the fuel cell output) needs to be higher than the power requirements (measured at the propeller). With the assumed combined electrical efficiencies, the power needs to be increased with around 10%, but engine room space limitations also apply. This combined effect results in installed powers of 9000, 1000 and 2400 kW for the ETV, RWS and MPV respectively.

5.4. Reformer systems

Element 1 is a producer of methanol reformer systems. Their design includes a membrane based hydrogen purifier, which separates hydrogen by passing it through a selective membrane, which happens due to a pressure difference between the two sides of the membrane. The resulting hydrogen stream is 99.97% pure, containing <0.2 ppm CO and <0.2 CO_2. This is pure enough for LTPEM applications (Cheng et al., 2007).

Recalling the main methanol steam reforming reaction:

$$CH_3OH + H_2O \rightarrow 3H_2 + CO_2 \tag{5.1}$$

For each mole of methanol (and one mole of water), three moles of hydrogen are produced. In the specification sheet, it is given that an input of 1.645 L/min feedstock results in 1.300 L/min hydrogen. The feedstock used is a 62.5/37.5 percent by weight methanol/water mixture. Using the molar mass of methanol and water, this equals a 68/32 percent by volume methanol/water mixture. Thus, 1.12 litres methanol is consumed per minute. Using the 1:3 molar ratio and the ratios of molar mass of methanol and hydrogen, this would result in 1.86 litres of hydrogen per minute. Dividing the actual flow by this number gives a membrane selectivity of 70%. This means that 70% of the produced hydrogen is available for fuel cells. The unpermeated hydrogen that remains in the retentate is combusted using oxygen to provide heat to the system. The combustion reaction of hydrogen is:

$$H_2 + \tfrac{1}{2}O_2 = H_2O \tag{5.2}$$

As the retentate also contained CO_2 and CO due to the main and side reforming reactions, this is also present in the exhaust stream. Oxygen is present as this was used to combust hydrogen. According to the manufacturer, the exhaust gas stream contains 12.7% oxygen, 5 ppm CO and no detectable NO and NO_x. An overall efficiency of up to 80% is reported. Each reformer module produces enough hydrogen for a 100 kW fuel cell system. The modules have a mass of 900 kilograms and a size of 1525/915/1980 mm (length/width/height).

5.5. Carbon capture

Hitherto no vessel is known to exists with a combination of (methanol) reformers and carbon capture. The only known related application case is the HyMethShip project, where a membrane reactor will be used to capture pure CO_2 from the reformer output. The CO_2 is then liquefied and stored on board, in either dedicated tanks or in dual purpose methanol/CO_2. The current status of this system is unknown, though preliminary publications suggest a 97% capture rate (Wermuth, Lackner, et al., 2020). Since this is the only reference project, this figure will be used as an assumption going forward.

However, it must be noted that the type of reformer used in this thesis is not the same as developed by the HyMethShip project, so the capture rate may not be realistic for this type of reformer.

5.5.1. CO_2 separation

The reformer system from Element 1 has an exhaust gas composition that includes steam and oxygen alongside CO_2. This is because the retentate is burned in order to provide heat to the system. If instead a larger membrane section, or even a membrane reactor altogether is used (such as in the HyMethShip project), which results in a more selective membrane, a pure CO_2 stream can be theoretically obtained. Since the hydrogen stream will also be larger and thus more electric energy can be produced in the fuel cells, this energy can be used to generate heat for the reformer systems instead of an integrated burner. The drawback is a lower reformer efficiency, but the CO_2 stream is easier to capture.

5.5.2. CO_2 flow rate

The maximum CO_2 flow that should be captured occurs at maximum power, when the methanol consumption and conversion is largest. Chemically speaking, one mole of methanol results in one mole of carbon dioxide, as discussed in Section 5.4. In terms of mass flow at maximum power demand, the following expression is used to find the maximum CO_2 capture rate:

$$\dot{m}_{CO_2,max} = \dot{m}_{CH_3OH,max} \cdot \frac{M_{CO_2}}{M_{CH_3OH}} = \frac{P_{max}}{\eta_{reformer} \cdot \eta_{FC} \cdot HHV_{CH_3OH}} \cdot \frac{M_{CO_2}}{M_{CH_3OH}} \tag{5.3}$$

For the three ship types, the CO_2 flows are therefore as follows:

$$\dot{m}_{CO_2,max}(\text{ETV}) = \frac{9000\ [\text{kWh}]}{0.8 \cdot 0.46 \cdot 5.53\ [\text{kWh/kg}]} \cdot \frac{44.01\ [\text{kg/mol}]}{32.04\ [\text{kg/mol}]} = 6075\ [\text{kg/h}] \tag{5.4}$$

$$\dot{m}_{CO_2,max}(\text{RWS70}) = \frac{1000\ [\text{kWh}]}{0.8 \cdot 0.46 \cdot 5.53\ [\text{kWh/kg}]} \cdot \frac{44.01\ [\text{kg/mol}]}{32.04\ [\text{kg/mol}]} = 675\ [\text{kg/h}] \tag{5.5}$$

$$\dot{m}_{CO_2,max}(\text{MPV}) = \frac{2400\ [\text{kWh}]}{0.8 \cdot 0.46 \cdot 5.53\ [\text{kWh/kg}]} \cdot \frac{44.01\ [\text{kg/mol}]}{32.04\ [\text{kg/mol}]} = 1620\ [\text{kg/h}] \tag{5.6}$$

5.5.3. Liquefying CO_2

The density of CO_2 varies with temperature and pressure. A higher density is reached under high pressure and low temperature, when CO_2 becomes liquefied. Liquid CO_2 is about 500 times more dense than gaseous CO_2 (Seo et al., 2015). Liquefying CO_2 can be done with a series of compressors and coolers, which can have different configurations (Jackson & Brodal, 2018). An electricity consumption of up to 250 kWh per tonne CO_2 was found (Lucquiaud et al., 2013), but not included in the model, as will be further mentioned in the discussion (Section 8.1).

5.6. Methanol storage

With methanol having a low energy density compared to MGO, more than twice the tank volume is needed for the same amount of energy. The required volume is further increased by rules, requiring methanol tanks to be surrounded by 900 mm cofferdams, except when next to bottom shell plating or other methanol tanks.

The minimum size of on-board methanol storage is determined by various factors. The most important one is vessel autonomy and endurance: the vessel must be able to complete its missions without refuelling. The second factor is bunkering capabilities and facilities. If every vessel's main

port of operations is equipped with a methanol bunkering station, refuelling can happen after every trip. But if dedicated refuelling trips must be made, larger on-board storage is preferable, as these trips would cost both time and more fuel.

As methanol reformers use deionised water to reform methanol into hydrogen, additional tanks are needed. The Element 1 reformers use a 62.5/37.5 percent by volume methanol/water ratio. This means that for every m^3 of methanol, 0.6 m^3 of water is needed. Water tanks do not need cofferdams, which also decreases the overall volume needed on board compared to methanol tanks.

5.6.1. ETV

The amount of methanol that the ETV must be able to carry is dependent on the operational profile that includes an emergency towing operation. In this case, the vessel needs enough methanol for 14 days of stand-by and a further 2 days of emergency towing. Depending on the amount of fuel cell systems operating together (which influences the overall efficiency), between 240 and 265 tonnes of methanol are needed for each trip if the operational profile is followed. As will become apparent in Section 6.2.1, the actual fuel consumption is usually much lower than the operational profile would indicate, but since the vessel should be able to follow at least this operational profile, the 265 tonnes are considered the minimum size. As fixed-size cofferdams are needed, it is most efficient to position the methanol tanks as close together as possible. The new tanks are positioned in the same general location as the original fuel tanks. Deionised water tanks should be included as well, with 60% capacity compared to methanol tanks, but without cofferdams. In total, the tanks depicted in Figure 21 can hold 394 m^3 or 312 tonnes of methanol, and 244 m^3 of deionised water.

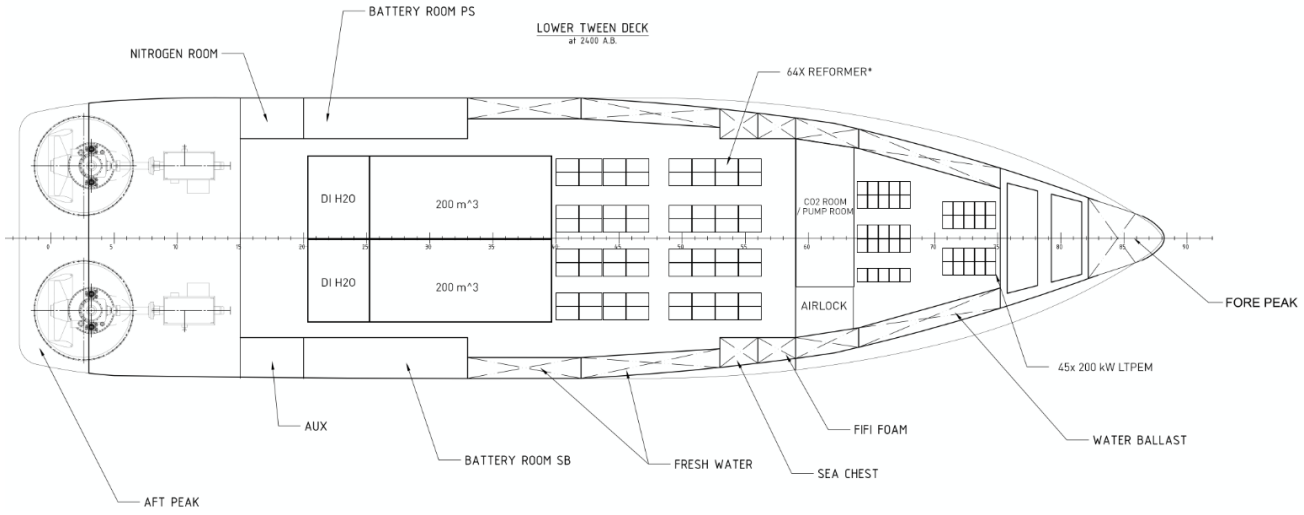

Figure 21: ETV lay-out, lower deck

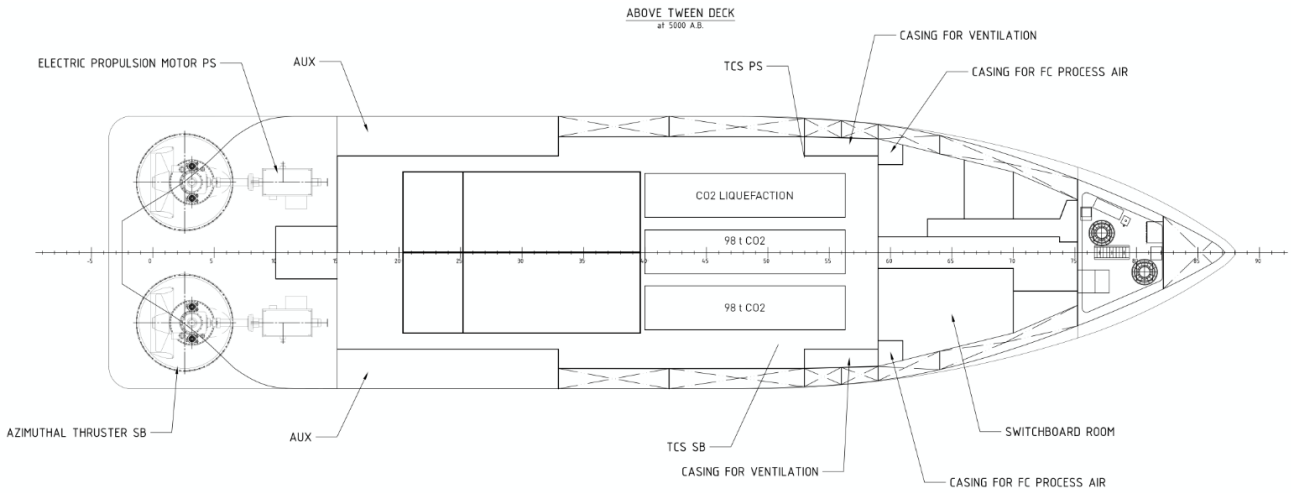

Figure 22: ETV lay-out, second deck

5.6.2. RWS70

According to an internal report on the user needs of Rijkswaterstaat patrol vessels, the highest energy demand without refuelling is 8.3 MWh, plus a bunker margin of 10 percent. Using the methanol lower heating value, this results in a minimum methanol storage of 1651 kilograms or 2.08 m^3:

$$V_{MeOH,min} = \frac{E_{demand}}{LHV_{MeOH} \cdot \rho_{MeOH}} \cdot 1.1 = \frac{8.3 \cdot 10^3 \text{ [kWh]}}{5.53 \text{ [kWh/kg]} \cdot 792 \text{ [kg/m}^3\text{]}} \cdot 1.1 = 2.08 \text{ [m}^3\text{]} \quad (5.7)$$

The current volumetric fuel capacity of the RWS70 is 7 m^3. When filled with MGO this is equivalent to 84 MWh of energy. However, this fuel is stored in two longitudinal tanks at the sides of the vessel, each being around 700 mm wide. Clearly, since 900 mm cofferdams would be needed if the MGO is replaced by methanol, these tanks cannot be reused. It is more space-efficient to equip the vessel with a single methanol, centralised tank that can be surrounded by cofferdams. Following the wishes of the Rijksrederij, the tank should have sufficient capacity for two days of operation. A methanol tank with a capacity of 4.4 m^3 is installed, surrounded on the sides and top by 900 mm cofferdams. The placement is halfway in the original engine room, as seen in Figure 23. This tank splits the engine room in two, with the propulsion system in the aft room, and a separate reformer and fuel cell room in the front. A separate hatch for this room needs to be installed, the back room is accessible from the original engine room entrance. Connections between fuel cells and electric motors can be fitted through the cofferdams.

For 4.4 m^3 of methanol, 2.64 m^3 of deionised water is needed. This water tank does not need cofferdams and is placed in the aft room and has a footprint of 3 by 0.8 metres. If the tank was square, a height of 1.1 metres is sufficient, but due to the shape of the hull a higher tank is needed. The available height in this part of the ship is 1.5 metres, sufficient to account for the shape of the hull in regard to water tank capacity.

The RWS70 has limited space, and the installed tank size limits the space left for other equipment. In fact, the Element 1 M13 methanol reformers are too big to be fitted on board, and only four out of ten systems that are needed fit. Therefore, the vessel needs to be either lengthened by around 1.8 metres, or the reformers need to be 2.5 times more compact in terms of footprint size. For the rest of this thesis, it is assumed that both the fuel cell and reformer systems will be more compact in the future, so that all systems will eventually fit in the ship. However, it must be noted that this is not possible with the current commercially available systems.

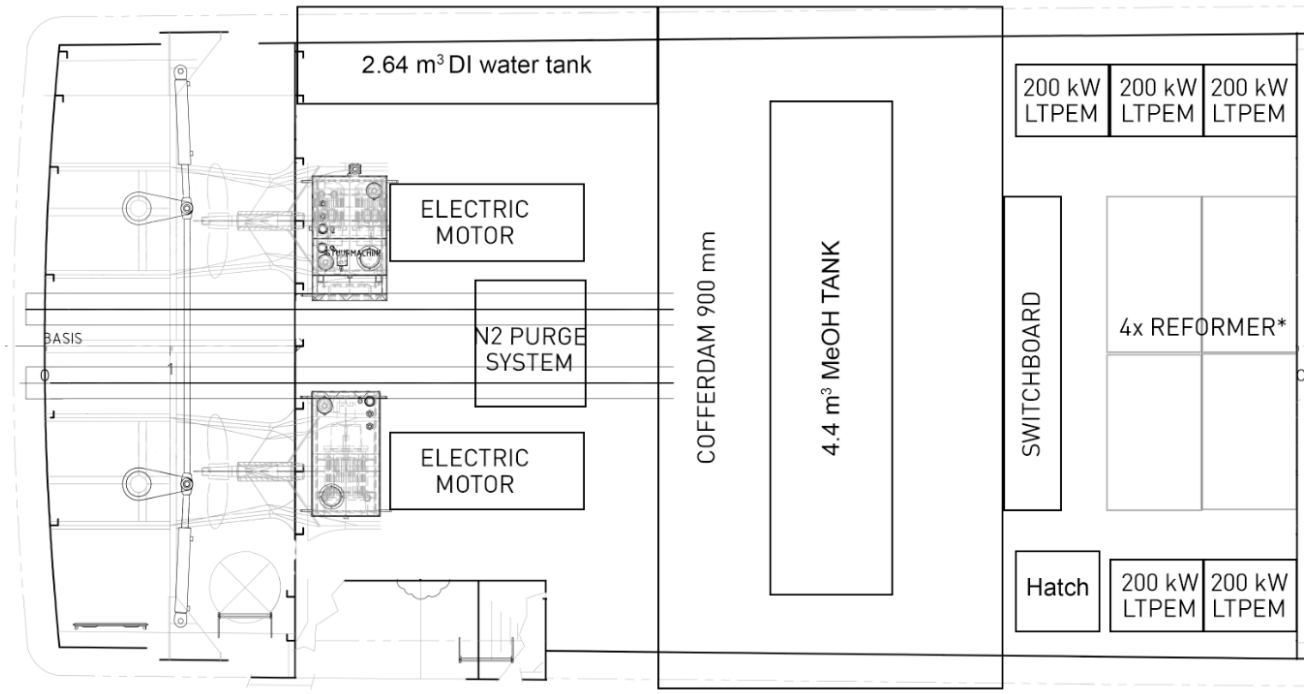

Figure 23: Proposed lay-out of the RWS70.

5.6.3. MPV

The MPV has three different main tasks. As every trip the vessel makes only one a single main task is performed, the model is used to determine which of these trips requires the highest amount of methanol storage. The result is that the "marking" task has the highest fuel consumption: approximately 20 tonnes of methanol and 12 tonnes of deionised water are needed. Therefore, these are the minimum tank sizes for the MPV.

If part of the tanks in the existing design were to be outfitted with 900 mm cofferdams, 25 tonnes of methanol are able to be stored on board, as seen in the confidential appendix. A water tank holding 15 tonnes of deionised water is also present to ensure enough available water for the reformer systems.

5.7. CO_2 storage

The minimum CO_2 storage capacity is calculated using the model, as described in Section 4.7. In general, these tanks should hold at least as much CO_2 as produced (and subsequently captured) during a single trip. However, for some vessels there can be different wishes from the owner in regard to the frequency of unloading these tanks, to avoid having to perform this operation almost daily.

Liquid CO_2 tanks are cylindrical. ISO container sized tanks (storing up to 19 tonnes of CO_2 in a 20 foot container (COMTECSWISS, n.d.)) are common, but bigger tanks exist. For example, ASCO offers 13.5 metre long tanks with a diameter of 3.2 metres, which can store up to 100 tonnes of liquid CO_2.

5.7.1. ETV

On a single deck of the ETV, three of the 100 tonne ASCO tanks are able to be installed, giving a 300 tonne CO_2 storage capacity. For a normal operational profile, even 200 tonnes is sufficient. Only in the case of trips with emergency towing operations, more storage would be needed. The trade-off between emissions and storage space is further discussed in Section 6.3.1.

5.7.2. RWS70

With its 24-hour operational profile, it is theoretically sufficient for the RWS70 to only have enough CO_2 storage capacity for a single day, as it can be unloaded in port daily. However, in correspondence with the wishes of the Rijksrederij, enough storage is needed for two days worth of CO_2. According to calculations done in the next chapter, daily CO_2 emissions are around 1.7 tonnes, so 2.4 tonnes worth of storage is needed. For this, a 3000 litre CO_2 tank is needed. On board of the RWS70, storage is possible on deck, in accordance with the Rijksrederij, making it theoretically possible to outfit the ship with a carbon capture and storage system.

5.7.3. MPV

As the “marking” main task requires the highest amount of methanol, this also results in the highest CO_2 output. During each trip up to 26 tonnes of CO_2 are produced. The existing design has space for two ISO sized CO_2 tanks (20 ft), in total holding 38 tonnes of CO_2, more than enough for a single trip. The position in the ship can be seen in the confidential appendix.

5.8. Nitrogen purge systems

A nitrogen system is present for safety reasons. It can be used to inert and purge fuel piping and fuel tanks. A SKID can be used to produce nitrogen on board, which can be stored in a buffer tank and distributed with pumps and compressors. According to class rules, nitrogen purge systems need to be 95% pure N_2 (DNV GL, 2020). Purge piping should lead to open air, regarded as outlet from hazardous zone. Further, more detailed designs are necessary in order to calculate the dimensions of all nitrogen related components.

6. Tank-to-propeller emissions

The model from the previous Chapter can now be used to calculate the tank-to-propeller emissions of different ships. The results from the on-board integration in Chapter 5 are used as input for the MATLAB-Simulink model from Chapter 4. As mentioned in previous sections, this is an iterative process, and some results of this Chapter were used during the on-board integration process. The goal of this Chapter is to give an estimate of the tank-to-propeller emissions of the three different ship types, based on several assumptions that will be discussed when relevant.

6.1. Operational profile

The operational profiles of the three different Rijksrederij vessels are be structured similarly. Each vessel in principle performs one main task per trip. Each main task is split into several subtasks, which are further specified by maximum and average power demands during each subtask.

6.1.1. ETV

The full operational profile for the emergency towing vessels is presented in Table 6. Each ETV is on standby most of the time (95%), of which the majority (75%) is spent in a low power standby mode. Full power is only needed during 20% of mobilising for standby tasks and during towing operations.

The vessel needs enough fuel for an autonomy of 14 days on standby, whilst keeping enough reserves for a 48-hour towing operation at all times. The total minimum fuel capacity is therefore dictated by the sum of capacity needed for both the standby and towing tasks.

Main task		**Subtask**		**Autonomy**	**Maximum power**		**Average power**	
Towing	**[5%]**	Mobilisation	[10%]	5 hrs	6000 kW	[20%]	1500 kW	[80%]
		Towing	[90%]	43 hrs	8000 kW	[30%]	5500 kW	[70%]
Standby	**[95%]**	Mobilisation	[25%]	84 hrs	8000 kW	[20%]	4000 kW	[80%]
		Standby	[75%]	252 hrs	750 kW	[20%]	500 kW	[80%]

Table 6: Operational profile of an Emergency Towing Vessel (ETV).

With this operational profile in combination with its current propulsion systems, the ETV Guardian was expected to use 3057 tonnes of MGO, or 255 tonnes monthly. However, the fuel usage turned out to be lower than expected, as in the first eight months of 2021 the average monthly fuel consumption was only 107 tonnes. The highest monthly consumption was 190 tonnes. These figures raise the question whether the current energy storage capacity of approximately 750 tonnes MGO is unnecessarily big. This was already taken into account when discussing the methanol tank size in Section 6.2.1.

6.1.2. RWS 70

As a fast patrol vessel that is on stand-by 24/7, the RWS 70 has a straightforward operational profile which can seen in in Table 7. The vessel has one main task: patrol. On average, the vessel spends 4 hours per day at maximum power, 14 hours per day between 15 and 75 kW, and 6 hours per day on shore power.

Main task	Subtask		Autonomy	Maximum power		Average power	
Patrol	Mobilisation/Patrol	[50%]	12 hrs	1000 kW	[30%]	75 kW	[70%]
	Manoeuvring	[25%]	6 hrs	15 kW	[100%]		
	Port	[25%]	6 hrs	0 kW	[100%]		

Table 7: Operational profile of the RWS 70

6.1.3. MPV

Inherent to its multi purpose capabilities, the MPV has a varied operational profile. Three main tasks are identified: marking of shipping lanes, measurement operations, and patrol/incidents. The maximum power demand is 2200 kW. Assuming the vessel only performs one main task per trip, storage tank sizes (of fuel and CO_2) must be sized according to the main task with the highest energy demand. This energy demand is calculated by multiplying the power levels with the time spent at these power levels. The "Marking" task demands the most power, so this task is used as an input for the tank-to-propeller model when calculating trip emissions and fuel consumption. When calculating the yearly figures, the full operational profile is used as input. A summary of this operational profile is found in Table 8.

Main task		Subtask		Autonomy	Maximum power		Average power	
Marking	**[80%]**	Mobilisation	[20%]	24 hrs	2200 kW	[10%]	1100 kW	[90%]
		Buoy handling*	[30%]	36 hrs	500 kW	[20%]	250 kW	[80%]
		Port	[50%]	60 hrs	150 kW	[20%]	50 kW	[80%]
Measuring	**[10%]**	Mobilisation	[20%]	24 hrs	2200 kW	[10%]	662 kW	[90%]
		Measuring*	[30%]	36 hrs	300 kW	[20%]	1100 kW	[80%]
		Port	[50%]	60 hrs	150 kW	[20%]	150 kW	[80%]
Patrol/incidents	**[10%]**	Mobilisation/patrol	[25%]	12 hrs	2200 kW	[30%]	50 kW	[70%]
		Manoeuvring	[75%]	36 hrs	300 kW	[50%]	649 kW	[50%]

Table 8: Operational profile of MPV 50. **: and/or manoeuvring*

6.2. Storage tank size

The storage tank size (methanol, deionised water and CO_2) is based on Simulink outputs for trip data. The figures that will be presented have the average efficiency on the x-axis. This efficiency range corresponds with the balancing of efficiency and lifetime as discussed in Section 4.4. It is up to the owner to choose a working point based on expected cost factors that were also discussed in that Chapter.

6.2.1. ETV

The visualised output from the Simulink model is presented in Figure 24. Here, it can be seen that a minimum of around 250 tonnes of methanol storage and just under 150 tonnes of deionised water is required. As mentioned earlier in the text, the current MGO tank capacity is higher than dictated by the operational profile, meaning that the vessel does not need to bunker after each trip. To save space on board, the fuel capacity can be lowered to the 250 tonnes that follows from the (16 day) operational profile, especially since in practice the vessel does not consume this much fuel in a month. This way, there can be enough fuel stored for at least two trips, though bunkering after every trip might be advisable.

Previous fuel storage capacity statements were on MGO. Since not only the fuel but also the power train (with different efficiencies) changes, calculating the required methanol storage is not a conversion solely based on the ratio of energy densities. Instead, a simulation is made coupling the operational profile to the systems with their efficiencies and power consumption at different load levels.

As mentioned in Section 5.7.1, the ETV sometimes requires extra methanol during a trip, when towing operations are required. If this happens at the end of a fourteen day trip, the total methanol exceeds the usual consumption, and thus the CO_2 output is also higher than normal. However, since this only happens sporadically, the decision is made to not take this edge case into account when dimensioning the CO_2 storage tanks. This decision will be further substantiated in Section 6.3.1, where the impact of this choice on yearly emissions is considered.

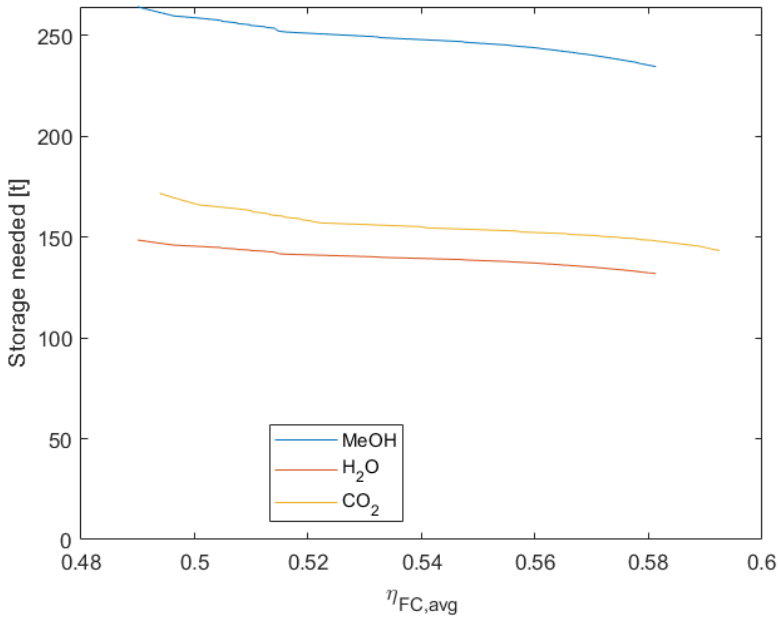

Figure 24: Required storage capacities for the ETV.

6.2.2. RWS70

The RWS 70 currently has two 3.25 tonne MGO tanks on board, sufficient for about 21 days of operation. Figure 25 shows that just under 2 tonnes of methanol are required, and around 1.1 tonnes of deionised water. If it is at all possible to fit carbon capture systems on board of the RWS70, the tanks should be able to hold at least 2.6 tonnes of CO_2 for a single trip.

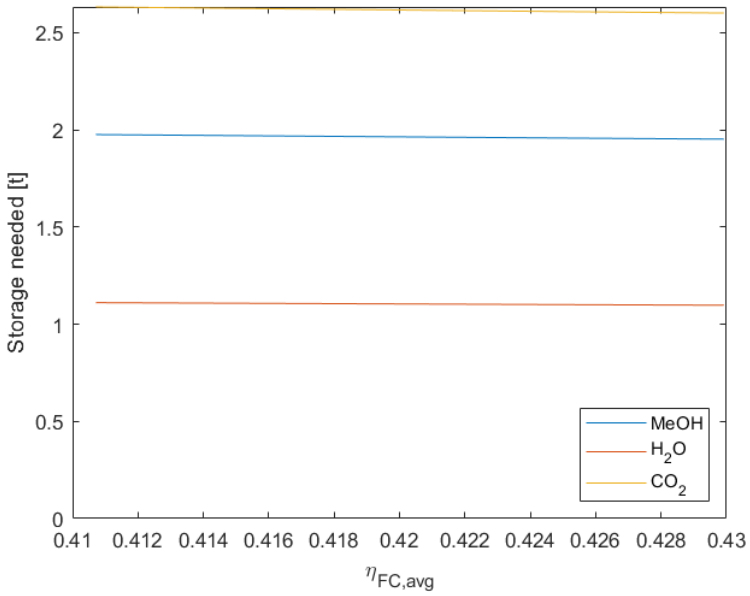

Figure 25: Required storage capacities for the RWS70.

6.2.3. MPV

As mentioned in Section 6.2.3, the fuel storage capacity is based on the “Marking” main task. Figure 26 shows minimum storage capacities of 20 tonnes of methanol, 11 tonnes of deionised water and around 25 tonnes of CO_2.

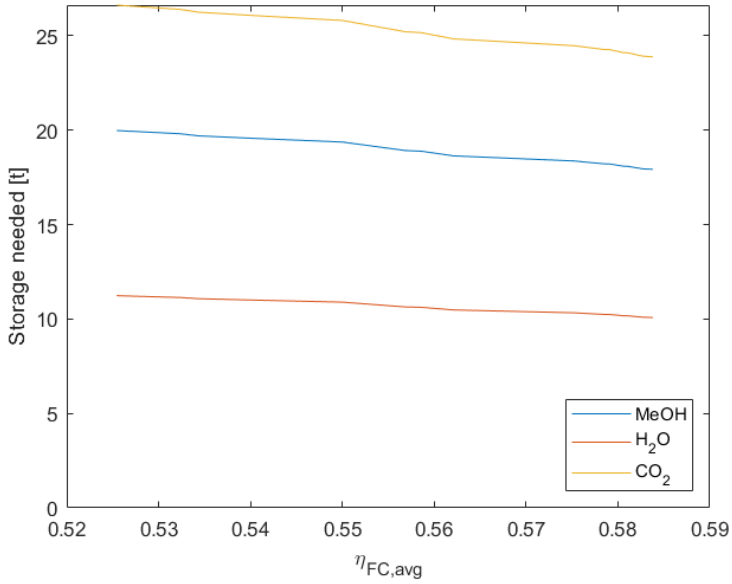

Figure 26: Required storage capacities for the MPV.

6.3. Yearly emissions

The yearly emissions are calculated using the tank-to-propeller model, with the estimated yearly operational hours in combination with the operational profile as input. For the RWS70 and MPV, all captured CO_2 can be stored during each trip, as these have sufficiently large CO_2 tanks. The ETV is a special case when considering tank capacity, which will be discussed below.

6.3.1. ETV

As mentioned before, more CO_2 storage space is needed during towing operations. In normal conditions, two 100 tonne tanks are enough, whilst in the most "CO_2-producing scenario" (i.e. full 14 days of stand-by and two days of towing) four tanks are needed. However, because these types of operations only happen sporadically, it is sensible to look at the impact on the total yearly emissions. Based on the yearly fuel consumption data, an estimation of number of trips with and without emergency towing was made, with a fixed fuel consumption per trip. Then, the model was used to predict the total emissions for all yearly "normal" trips (without emergency towing), and the total emissions for all yearly "emergency" trips (trips including emergency towing operations). This was done for different on-board storage capacities, as this is a variable model parameter. The CO_2 output was split in three categories: emissions due to slip (as not 100% of the CO_2 can be captured), emissions due to tank capacity limit and captured CO_2. The results are visualised in Figure 27, where the results for two tanks, three tanks and four tanks are shown. For two tanks, 382 tonnes of CO_2 are emitted yearly. For three tanks, this is roughly halved: 186 tonnes. For three tanks, 131 tonnes of CO_2 are still emitted due to slip.

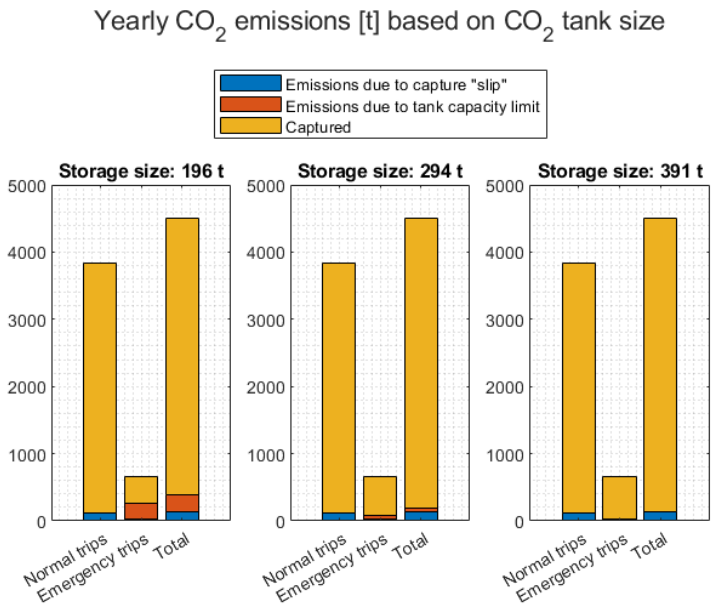

Figure 27: Yearly CO_2 emissions and captured CO_2 of the ETV, based on different storage capacities.

6.3.2. RWS70 & MPV

Based on the yearly operational hours (around 2000) and the operational profile, 217 tonnes of CO_2 are produced annually. If carbon capture is possible with a large enough tank capacity (3000 litres, see 5.7.2), 200 tonnes of this are captured (with the assumed capture ratio), and 17 tonnes are emitted. The MPV produces 1392 tonnes of CO_2 (based on 5300 operational hours), of which 1351 tonnes are captured and recycled. This leaves 41 tonnes of CO_2 emissions per year.

7. Well-to-propeller emissions

The previous Chapters have dealt with the well-to-tank and tank-to-propeller emissions of three ship types. However, to answer the main research questions, the results need to be extended to reflect the well-to-propeller emissions of the entire fleet. This involves two main aspects: the energy demand of the entire fleet and the total emissions if renewable methanol is used to fulfil this energy demand. Then, it can be answered whether or not it is possible to fuel the Rijksrederij fleet with renewable methanol fuel cells, which was the premise of the main research question:

"To what extent can fuel cells and renewable methanol be used to eliminate the well-to-propeller greenhouse gas emissions of the Rijksrederij fleet?"

7.1. Fleet energy demand

A previous analysis by the Rijksrederij was used to construct a list of vessels that are projected to sail on methanol (in combustion engines) in 2030. Other ships will be sailing on other renewable sources of energy, such as hydrogen and electricity. Apart from the vessel types that were further looked into in this thesis, the methanol-fuelled fleet will consist of various multi-purpose vessels, patrol vessels and Rigid Hull Inflatable Boats (RHIBs). The full range of vessels with some of their specifications and yearly methanol is listed in Table 9. The methanol demand for the first three ships types follows from the calculations done in the previous sub questions, for the other ships they are based on estimations of the Rijksrederij.

Vessel	No. of vessels	Length	Displacement	Installed power	Methanol demand (tot.)
ETV	3	66 m	4000 t	8900 kW	8913 t
MPV-50	4	50 - 60 m	1200 t	2200 kW	3684 t
RWS70	10	24 m	67 t	1000 kW	1630 t
MPV-200	2	60 m	2000 t	3500 kW	3062 t
MPV-100	1	75 m	3000 t	2500 kW	2432 t
MPV-50 A1	1	75 m	3500 t	3000 kW	1081 t
Patrol vessel 1B	3	15 m	20 t	1000 kW	378 t
Patrol vessel 2B	11	18 m	25 t	1000 kW	1398 t
Patrol vessel 3B	7	22 m	35 t	1500 kW	897 t
RHIB	6	10 m	3 t	300 kW	152 t

Table 9: Overview of different methanol-fuelled vessels in 2030

7.2. Methanol supply

As discussed in Chapter 2, the bio-methanol pathways are considered carbon neutral in the well-to-tank cycle, if carbon sequestration is considered. The green methanol pathway is carbon neutral in the well-to-propeller cycle, as the CO_2 needs to be recycled using on-board carbon capture. As not all CO_2 can be recovered from the fleet, solely relying on green methanol would already result in positive CO_2 emissions. Therefore, the green methanol pathways are preferrable, as this leaves room to emit some CO_2 from the fleet while still operating carbon neutral. As bio-methanol can not cover the entire methanol demand, it still needs to be combined with green methanol.

The choice between both bio-methanol pathways is a practical one. Both pathways rely on the same amount of biomass and are able to produce more or less the same amount of methanol. However, there are two arguments for the pathway using mono-fermentation. The first argument is that Rijkswaterstaat is already planning to use biomass in mono-fermentation to produce biogas, and it is thus projected that the CO_2 to produce methanol will be available. Secondly, this pathway uses CO_2 hydrogenation to produce methanol, which is the same technique as green methanol uses. CO_2 streams from mono-fermentation and from on-board capture can therefore be combined in the same methanol production facility, combined with hydrogen produced using wind energy. This in contrast to the second bio-methanol pathway, which uses gasification of biomass to produce methanol directly.

In short, a combination of mono-fermentation derived bio-methanol and green methanol is preferred, both produced using the same hydrogenation facility. The preferred mix is leaning towards as much bio-methanol as possible, because of its carbon neutral status without on-board carbon capture. Since this process also requires electricity, less green methanol is available when compared to the table presented in Section 0. Table 10 shows the proposed fuel mix for the Rijksrederij fleet, with all hydrogen and CO_2 sources and the amount of methanol that can be produced using this combination.

	Bio-methanol (1)	**Green methanol**	**Total**
Hydrogen feedstock	Wind energy	Wind energy	Wind energy
Electrolyser power consumption	24 GWh	214.4 GWh	238.4 GWh
H_2 produced/consumed	482 t	4254 t	4767 t
Carbon feedstock	Mono fermentation of biomass*	On-board CO_2 capture	Both
Biomass consumed	15000 t*		15000 t*
CO_2 consumed	3500 t	29201 t	34391 t
Production power consumption	0.36 GWh	11.3 GWh	11.66 GWh
Net CO_2 emissions	-2995 t	4212 t	1217 t
Maximum methanol production	2064 t	17219 t	19283 t

Table 10: Proposed fuel mix for the Rijksrederij fleet.

One noteworthy point is the supply of CO_2 to produce green methanol. If too much CO_2 is emitted instead of captured, there is not enough available for production, and a different CO_2 source is needed. The net CO_2 emissions can then only be zero if this source is considered carbon negative in itself (like biomass). This is another argument for combining both bio-methanol and green methanol: the well-to-tank emissions are negative, leaving some room for positive emissions in the tank-to-propeller section. However, since the process of producing green methanol also emits CO_2, and this is not offset enough by the negative CO_2 emissions from using biomass in bio-methanol production, the overall methanol production is already carbon positive. No amount of carbon capture can push this to zero or negative total emissions, especially since 100% capture rate can not be achieved. Therefore, other carbon negative sources (such as direct air capture or more biomass-derived CO_2) need to be used.

The above conclusions are visualised in Figure 28, which is a diagram showing all CO_2 flows that are considered in this thesis. The blue lines represent CO_2, the orange part is the conversion to and from methanol (respectively during methanol production and methanol reforming on board). The diagram shows the case where the sum of production losses and exhaust losses is greater than the amount of CO_2 derived from biomass. This results in positive well-to-tank emissions as well as a production gap: to ensure a constant annual methanol flow, more (external) CO_2 is needed. Ways to reach net-zero emissions will be discussed in Section 7.4.

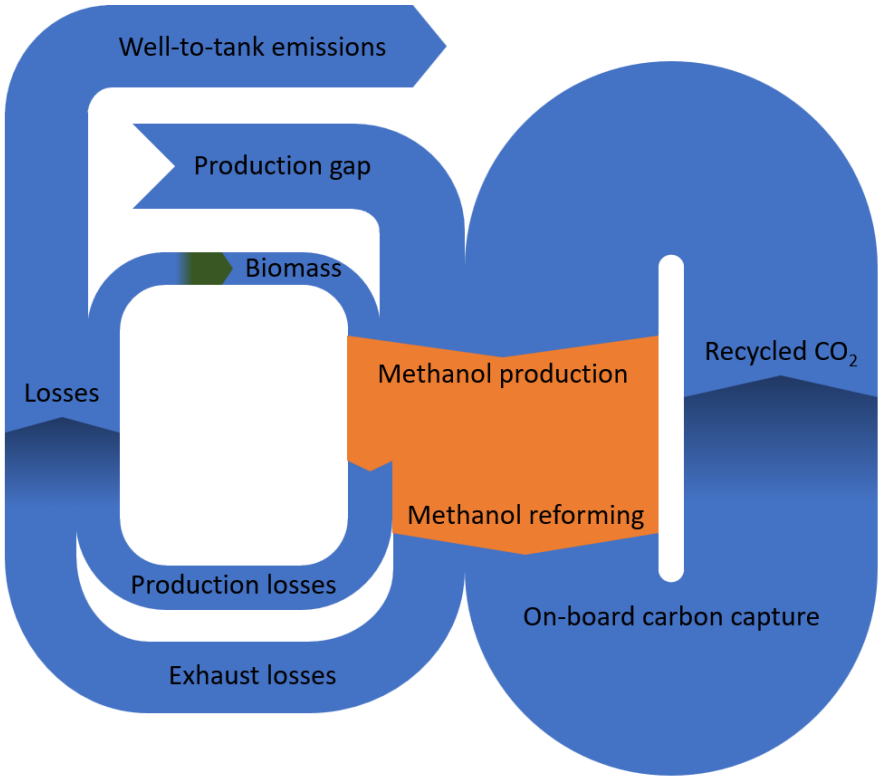

Figure 28: Diagram showing CO_2 flows (not to scale) taken into account in the well-to-tank emission analysis.

7.3. Well-to-propeller emissions

The calculation of total well-to-propeller emissions is the sum of emissions from the various sub-processes. The methanol-fuelled part of the fleet as discussed in Section 7.1 is considered. Together with the expected energy demand and efficiency of fuel cell systems, a yearly methanol consumption is calculated. Some vessels are expected to be able to use on-board carbon capture systems, others are not. Estimations are made based on ship lay-outs, dimensions and comparisons to the vessels considered in this thesis. This results in a list of vessels with corresponding CO_2 emissions and amount of captured CO_2. This can be cross-referenced with the methanol supply and corresponding emission values from Section 7.2 to obtain the total well-to-propeller emissions.

The vessel types that are projected to use methanol in 2030 are mainly multi-purpose and patrol vessels, both of various sizes. The smaller vessels are not expected to be able to allow carbon capture systems to fit, as this was already a problem on the RWS70 (where deck space was needed for these systems – something that is not possible on vessel smaller than this). Table 11 shows the projected recovered and emitted CO_2 for the whole fleet. When comparing the total methanol demand to the total supply from Table 10, a gap of 3225 tonnes is present. This is due to the loss of CO_2 on-board: since not all CO_2 can be recovered from the used methanol, less new green methanol can be made. The tank-to-propeller emissions in Table 11 are added to the well-to-propeller emissions of Table 10, resulting in a total well-to-tank emission of 7164 tonnes annually, as seen in Table 12.

Vessel	No. of vessels	Methanol demand	CO_2 captured	CO_2 emitted
ETV	3	8913 t	10560 t	1308 t
MPV-50	4	3684 t	5404 t	164 t
RWS70	10	1630 t	1997 t	173 t
MPV-200	2	3062 t	3757 t	326 t
MPV-100	1	2432 t	2983 t	259 t
MPV-50 A1	1	1081 t	1326 t	115 t
Patrol vessel 1B	3	378 t	0 t	504 t
Patrol vessel 2B	11	1398 t	0 t	1864 t
Patrol vessel 3B	7	897 t	0 t	1196 t
RHIB	6	152 t	0 t	152 t
Total		***22508 t***	***29201 t***	***5947 t***

Table 11: Total fleet methanol demand, captured CO_2 and tank-to-propeller CO_2 emissions.

Vessel	Net CO_2 emissions
Bio-methanol carbon source	-3500 t
Bio-methanol production loss	505 t
Green methanol carbon source	0 t
Green methanol production loss	4212 t
Fleet emissions	5947 t
Total	***7164 t***

Table 12: Total annual well-to-propeller emissions.

7.4. Pathways to net zero well-to-propeller emissions

In conclusion, the methods presented in this thesis do not result in net zero well-to-propeller CO_2-emissions for the Rijksrederij fleet, but rather in positive emissions. As explained in Section 7.2, there is also a production gap regarding the supply of CO_2 to produce methanol. If these two paths (the losses and production gap) can be connected in some way, it is possible to produce enough methanol in a renewable way. This can be done by using a carbon negative source to close the production gap. This can be either more biomass-derived CO_2, or from advanced sources such as Direct Air Capture (DAC). This way, any losses from the system presented in Figure 28 are compensated by capturing CO_2 from outside the system, either directly (DAC) or indirectly (biomass).

Other ways to reach net-zero well-to-propeller emissions are to prevent or reduce losses in the first place, which would also prevent having a production gap. Performing carbon capture in the green methanol production process falls outside the scope of this project, but this is a step of the well-to-propeller emissions that contributes to around 40% of the total positive emissions – so there is a lot to gain in this step. The emission balance is also improved if the ratio of captured CO_2 on board is higher, for which technology needs to be more mature. Lastly, being able to equip the smaller vessels with CO_2 capture systems as well would be a big improvement, which would probably require lengthening the vessels if no major steps in power density of systems are made within the next few years.

8. Conclusion

The main research question of this thesis was:

"To what extent can fuel cells and renewable methanol be used to eliminate the well-to-propeller greenhouse gas emissions of the Rijksrederij fleet?"

The following sub questions were answered in order to obtain an answer to the main question:

1. *What pathways using Rijkswaterstaat's own resources can be used to produce renewable methanol in order to reduce or eliminate the well-to-tank greenhouse gas emissions?*

Three main pathways were identified:

- Combining by-product CO_2 from mono fermenting grass biomass, and hydrogen produced using wind energy, to produce bio-methanol (bio-methanol 1),
- Directly gasifying grass biomass to obtain bio-methanol (bio-methanol 2),
- Using on-board carbon capture to recycle CO_2, and produce green methanol by combining it with hydrogen produced using wind energy.

It was calculated that these options would result in annual production capacities of respectively 2064, 2152 and 20177 tonnes. The first two options use the same biomass source, so they can not be used together. Using the green methanol pathway together with one of the bio-methanol options is possible, but limited by the hydrogen production from the available wind energy. The well-to-tank emissions of the green methanol options are negative, as the biomass source is considered a carbon negative source, and any carbon emitted during the production process is sequestered over time. For green methanol they are positive, as even though the captured CO_2 is recycled (producing a closed, neutral CO_2 cycle), further emissions during the production process contribute to net positive emissions.

2. *How can the tank-to-propeller greenhouse gas emissions of a methanol fuel cell powered ship be calculated?*

A model was constructed to calculate the tank-to-propeller emissions of a methanol fuel cell powered ship. The main inputs of the model are operational and system parameters, which are all variables that can be changed depending on the vessel type that is analysed. The output gives information on the total methanol consumption, CO_2 output (including amount of captured CO_2, if the vessel allows for carbon capture) and costs. Consumption and CO_2 data is calculated both per trip and per year. This information can be used to iterate a vessels' design in order to achieve a higher efficiency or lower costs.

3. *How can methanol fuel cells and a carbon capture system be integrated into a Rijksrederij ship?*

Three ship types were identified to analyse in more detail: an emergency towing vessel (ETV), a patrol vessel (RWS70) and a multi purpose vessel (MPV). It was found possible to use methanol reformers on board, which produce hydrogen and CO_2. The hydrogen is fed to high temperature PEM fuel cells to produce electric energy, and the CO_2 can partially be captured and stored on board. The fuel capacity of all ships is lower than before (as methanol is less energy dense than traditional fuels, and water is needed for the reformers), but the ships are still able to perform their operational profile without running out of fuel.

Now, the main question could be answered, as both the well-to-tank and tank-to-propeller emissions were known. The answer to the third sub question was extended to an analysis on the fleet that the Rijksrederij is expecting to be able to operate on methanol in 2030. A choice was made in pathways to produce methanol: a combination of the first bio-methanol option and green methanol was found most interesting to the Rijksrederij. The total net CO_2 emissions of the methanol powered part of the fleet are presented in Table 13. The positive emissions of green methanol production are partially offset by the negative emissions of bio-methanol. However, the tank-to-propeller emissions are also positive, as not all CO_2 can be captured on-board. Therefore, even in the scenario where every methanol-fuelled ship can use on-board carbon capture, there will be net positive CO_2 emissions. The only ways to reach net-zero emissions is by improving the green methanol production process to not emit (as much) CO_2, improving the overall on-board capture ratio or a combination thereof. Otherwise, the CO_2 emissions must be compensated elsewhere, for example by using more waste biomass to produce methanol, or by using Direct Air Capture of CO_2.

Vessel	**Net CO_2 emissions**
Bio-methanol carbon source	-3500 t
Bio-methanol production loss	505 t
Green methanol carbon source	0 t
Green methanol production loss	4212 t
Fleet emissions	5947 t
Total	***7164 t***

Table 13: Total annual well-to-propeller emissions.

8.1. Discussion

A note must be made about the available wind energy. In the calculations for the part of the Rijksrederij fleet that is expected to be powered by methanol, it was assumed that all of the 250 GWh of wind energy could be used for this specific part of the fleet. However, this energy is reserved for the entire fleet, consisting of vessels possibly running on hydrogen or batteries in the future. Since this also requires electricity, this interferes with the conclusions made based on only part of the fleet. To meet the total energy demand, either more wind energy capacity is needed, or different renewable energy sources should be sought. The latter can also mean other (waste) biomass streams being used to directly produce methanol, which in this thesis was referred to as the second bio-methanol option.

A key element in this thesis was the ability of the Rijksrederij ships to perform on-board carbon capture. Since no practical implementations were found of carbon capture being performed on board of ships using methanol steam reformers, this part was based on a few assumptions. The HyMethShip project reported a 97% capture ratio, but this project is developing membrane reactors to reach this number, instead of the 'conventional' steam reformers referenced in this thesis. However, since no further data (including dimensions) of the membrane reactors were available, the data from the M13 reformers was used in both the tank-to-propeller model parameters and the integration on board of Rijksrederij ships. This is a gross assumption, as the M13 reformers have exhaust streams containing oxygen besides CO_2, as the reformer-off gases (hydrogen and CO_2) are burned in order to provide heat to the system. To make this type of reformer suitable for carbon capture, a more pure CO_2 stream is necessary, which could be achieved by extending the membrane section. This could make

the systems larger. However, since the size of the M13 systems has already decreased in the past few years, this enlargement may be offset by making other components smaller. Thus, it was chosen to retain the current M13 dimensions whilst still assuming the 97% capture rate.

Furthermore, there was a lack of data on dimensions of carbon capture systems. On the one hand, this was – again – due to the fact that no similar combination of systems (methanol reformers and carbon capture) is known to exist outside of preliminary research. On the other hand, whilst efforts were made to obtain data of similar non-maritime systems, the amount of gathered data was still too limited in order to provide more in-depth analyses on dimensioning of these systems, without completely stepping outside the scope of this research. The same problems arose with the carbon liquefaction systems: a figure of power consumption was only found in a late stage of the thesis, at a point where it was no longer possible to implement this figure in the model.

8.2. Recommendations

Recommendations for further research are directed two ways: academic research and research by the Rijksrederij, although this goes hand in hand. In the first category, more research is necessary towards carbon capture using methanol reformers. As discussed before, gaps exist when researching this combination, specifically in dimensioning the required systems. It should also be further researched if and how carbon capture is possible using 'conventional' methanol reformers like the Element 1 M13, and compare these findings to membrane reactors such as developed in the HyMethShip project. It should also be considered if a higher capture ratio is possible, in order to prevent CO_2 slip when sailing and to work towards a 100% carbon recycle rate. For the Rijksrederij it is recommended to further investigate the technical implementation on board of their ships. More detail is necessary in the aforementioned systems, which will have to stem from academic research and product development. In later stages, more detailed design is needed regarding piping and specific classification rules of each individual component. Furthermore, methanol production methods should be further researched with the specific feedstocks in mind. Especially ways to reduce the CO_2 emissions from methanol production should be considered, as this is a large contributor to the overall positive well-to-propeller emissions. Together with improving the on-board carbon capture rate this can help to get the Rijksrederij to net zero CO_2 emissions.

The model constructed in MATLAB-Simulink can be further improved in several ways. Firstly, as mentioned in the discussion, power consumption for CO_2 capture and liquefaction was not included due to time constraints. The impact of including this in the analysis would be an increased methanol consumption, except if batteries are included in the ship integration. These batteries are also something that should future research needs to include, as these can improve the power systems in multiple ways: including but not limited to dynamic load balancing, boosting at peak power demand (which may decrease the desired installed fuel cell power on some ships) and backup power. Hybrid battery and fuel cell powered ships can be a research topic of itself, as this configuration can allow for an increase in overall system efficiency.

Finally, a proper Life Cycle Analysis should be used to get a more detailed image of all emissions related to the production of renewable methanol and its use on board of fuel cell ships that perform carbon capture. Aspects that were not considered in this thesis, but can be taken into account in an LCA, include transportation costs of feedstocks and fuel, harvesting biomass (whilst considering if the biomass used is truly 'waste' biomass), and emissions of other compounds during every stage of the fuel lifecycle (for example during transport). Such LCA's can also be used to properly compare the performance of the pathways proposed in this thesis to other solutions, including other renewable fuels.

References

Alias, M. S., Kamarudin, S. K., Zainoodin, A. M., & Masdar, M. S. (2020). Active direct methanol fuel cell: An overview. *International Journal of Hydrogen Energy*, *45*(38), 19620–19641. https://doi.org/10.1016/j.ijhydene.2020.04.202

Allen, M. R., Dube, O. P., Solecki, W., Aragón-Durand, F., Cramer, W., Humphreys, S., Kainuma, M., Kala, J., Mahowald, N., Mulugetta, Y., Perez, R., Wairiu, M., & Zickfeld, K. (2018). Framing and Context. In *Global Warming of 1.5°C. An IPCC Special Report on the impacts of global warming of 1.5°C above pre-industrial levels and related global greenhouse gas emission pathways, in the context of strengthening the global response to the threat of climate change,*.

Atsbha, T. A., Yoon, T., Seongho, P., & Lee, C. J. (2021). A review on the catalytic conversion of CO2using H2for synthesis of CO, methanol, and hydrocarbons. *Journal of CO2 Utilization*, *44*(November 2020), 101413. https://doi.org/10.1016/j.jcou.2020.101413

Blumberg, T., Morosuk, T., & Tsatsaronis, G. (2017). Exergy-based evaluation of methanol production from natural gas with CO2 utilization. *Energy*, *141*, 2528–2539. https://doi.org/10.1016/j.energy.2017.06.140

Bozzano, G., & Manenti, F. (2016). Efficient methanol synthesis: Perspectives, technologies and optimization strategies. *Progress in Energy and Combustion Science*, *56*, 71–105. https://doi.org/10.1016/j.pecs.2016.06.001

Burhan, H., Cellat, K., Yılmaz, G., & Şen, F. (2021). Chapter 3 - Direct Methanol Fuel Cells. In *Direct Liquid Fuel Cells* (pp. 71–94). https://doi.org/https://doi.org/10.1016/B978-0-12-818624-4.00003-0

Carbon Recycling International. (n.d.). *The George Olah Renewable Methanol Plant*. Retrieved May 10, 2021, from https://www.carbonrecycling.is/projects#project-goplant

Cheng, X., Shi, Z., Glass, N., Zhang, L., Zhang, J., Song, D., Liu, Z. S., Wang, H., & Shen, J. (2007). A review of PEM hydrogen fuel cell contamination: Impacts, mechanisms, and mitigation. *Journal of Power Sources*, *165*(2), 739–756. https://doi.org/10.1016/j.jpowsour.2006.12.012

Cimenti, M., & Hill, J. M. (2009). Thermodynamic analysis of solid oxide fuel cells operated with methanol and ethanol under direct utilization, steam reforming, dry reforming or partial oxidation conditions. *Journal of Power Sources*, *186*(2), 377–384. https://doi.org/10.1016/j.jpowsour.2008.10.043

COMTECSWISS. (n.d.). *CO2-ISO Container*. http://www.comtecswiss.com/en/equipment-and-plants/co2-iso-container/

Dalena, F., Senatore, A., Marino, A., Gordano, A., Basile, M., & Basile, A. (2018). Methanol Production and Applications: An Overview. In *Methanol: Science and Engineering* (pp. 3–28). Elsevier B.V. https://doi.org/10.1016/B978-0-444-63903-5.00001-7

Das, S. K., Reis, A., & Berry, K. J. (2009). Experimental evaluation of CO poisoning on the performance of a high temperature proton exchange membrane fuel cell. *Journal of Power Sources*, *193*(2), 691–698. https://doi.org/10.1016/j.jpowsour.2009.04.021

Degnan, T. (2017). Transforming excess electricity and CO2 into “regenerative methanol.” *Focus on Catalysts*, *2017*(10), 1. https://doi.org/10.1016/j.focat.2017.09.001

Dicks, A. L., & Rand, D. A. J. (2018a). Direct Liquid Fuel Cells. In *Fuel Cell Systems Explained* (pp. 157–185). https://doi.org/10.1002/9781118706992.ch6

Dicks, A. L., & Rand, D. A. J. (2018b). Efficiency and Open Circuit Voltage. In *Fuel Cell Systems Explained* (pp. 27–41). https://doi.org/10.1002/9781118878330.ch2

Dicks, A. L., & Rand, D. A. J. (2018c). Introducing Fuel Cells. In *Fuel Cell Systems Explained* (pp. 1–26). https://doi.org/10.1002/9781118706992.ch1

Dicks, A. L., & Rand, D. A. J. (2018d). Solid Oxide Fuel Cells. In *Fuel Cell Systems Explained* (pp. 235–261). https://doi.org/https://doi-org.tudelft.idm.oclc.org/10.1002/9781118706992.ch9

Diéguez, P. M., Ursúa, A., Sanchis, P., Sopena, C., Guelbenzu, E., & Gandía, L. M. (2008). Thermal performance of a commercial alkaline water electrolyzer: Experimental study and mathematical modeling. *International Journal of Hydrogen Energy*, *33*(24), 7338–7354. https://doi.org/10.1016/j.ijhydene.2008.09.051

Diesveld, B., de Maeyer, E., & Diesveld, B. (2020). Maritime fuel cell applications: A tool for conceptual decision making. *International Shipbuilding Progress*, *67*(1), 53–73. https://doi.org/10.3233/ISP-190275

Dieterich, V., Buttler, A., Hanel, A., Spliethoff, H., & Fendt, S. (2020). Power-to-liquid via synthesis of methanol, DME or Fischer–Tropsch-fuels: a review. *Energy and Environmental Science*, *13*(10), 3207–3252. https://doi.org/10.1039/d0ee01187h

DNV GL. (2020). Pt.6 Ch.2. Propulsion, power generation and auxiliary systems. In *Rules for classification: Ships — DNVGL-RU-SHIP* (Issue July).

Ghasemzadeh, K., Harasi, J. N., Amiri, T. Y., Basile, A., & Iulianelli, A. (2020). Methanol steam reforming for hydrogen generation: A comparative modeling study between silica and Pd-based membrane reactors by CFD method. *Fuel Processing Technology*, *199*(November 2019), 106273. https://doi.org/10.1016/j.fuproc.2019.106273

Gurau, V., Ogunleke, A., & Strickland, F. (2020). Design of a methanol reformer for on-board production of hydrogen as fuel for a 3 kW High-Temperature Proton Exchange Membrane Fuel Cell power system. *International Journal of Hydrogen Energy*, *45*(56), 31745–31759. https://doi.org/10.1016/j.ijhydene.2020.08.179

Herdem, M. S., Sinaki, M. Y., Farhad, S., & Hamdullahpur, F. (2019). An overview of the methanol reforming process: Comparison of fuels, catalysts, reformers, and systems. *International Journal of Energy Research*, *43*(10), 5076–5105. https://doi.org/10.1002/er.4440

Jackson, S., & Brodal, E. (2018). A comparison of the energy consumption for CO2 compression process alternatives. *IOP Conference Series: Earth and Environmental Science*, *167*(1). https://doi.org/10.1088/1755-1315/167/1/012031

Kim, S., Yun, S. W., Lee, B., Heo, J., Kim, K., Kim, Y. T., & Lim, H. (2019). Steam reforming of methanol for ultra-pure H2 production in a membrane reactor: Techno-economic analysis. *International Journal of Hydrogen Energy*, *44*(4), 2330–2339. https://doi.org/10.1016/j.ijhydene.2018.08.087

Kleen, G., & Padgett, E. (2021). *DOE Hydrogen and Fuel Cells Program Record: Durability-Adjusted Fuel Cell System Cost*. *Dm*, 1–6. http://www.hydrogen.energy.gov/pdfs/9014_hydrogen_storage_materials.pdf

Kundu, A., Shul, Y. G., & Kim, D. H. (2007). Chapter Seven - Methanol Reforming Processes. In *Advances in Fuel Cells* (Vol. 1). Elsevier Ltd. https://doi.org/10.1016/S1752-301X(07)80012-3

Lee, B., Lee, H., Lim, D., Brigljević, B., Cho, W., Cho, H. S., Kim, C. H., & Lim, H. (2020). Renewable methanol synthesis from renewable H2 and captured CO2: How can power-to-liquid technology be economically feasible? *Applied Energy*, *279*(February). https://doi.org/10.1016/j.apenergy.2020.115827

Liu, Y., Li, G., Chen, Z., Shen, Y., Zhang, H., Wang, S., Qi, J., Zhu, Z., Wang, Y., & Gao, J. (2020). Comprehensive analysis of environmental impacts and energy consumption of biomass-to-methanol and coal-to-methanol via life cycle assessment. *Energy*, *204*, 117961. https://doi.org/10.1016/j.energy.2020.117961

Lucquiaud, M., Liang, X., Errey, O., Chalmers, H., & Gibbins, J. (2013). Addressing technology uncertainties in power plants with post-combustion capture. *Energy Procedia*, *37*, 2359–2368. https://doi.org/10.1016/j.egypro.2013.06.117

Lytkina, A. A., Orekhova, N. v., Ermilova, M. M., Petriev, I. S., Baryshev, M. G., & Yaroslavtsev, A. B. (2019). Ru-Rh based catalysts for hydrogen production via methanol steam reforming in conventional and membrane reactors. *International Journal of Hydrogen Energy*, *44*(26), 13310–13322. https://doi.org/10.1016/j.ijhydene.2019.03.205

Ministerie van Infrastructuur en Waterstaat. (2020). *CO_2-Managementplan 2020-2021*.

NEL. (2020). *M series containerized PEM electrolyser*. 116–117. https://nelhydrogen.com/wp-content/uploads/2020/03/Electrolysers-Brochure-Rev-C.pdf

Nieminen, H., Laari, A., & Koiranen, T. (2019). CO2 hydrogenation to methanol by a liquid-phase process with alcoholic solvents: A techno-economic analysis. *Processes*, *7*(7), 1–24. https://doi.org/10.3390/pr7070405

Papavasiliou, J., Avgouropoulos, G., & Ioannides, T. (2012). CuMnOx catalysts for Internal Reforming Methanol Fuel Cells: Application aspects. *International Journal of Hydrogen Energy*, *37*(21), 16739–16747. https://doi.org/10.1016/j.ijhydene.2012.02.124

Peppley, B. A., Amphlett, J. C., Kearns, L. M., & Mann, R. F. (1999a). Methanol-steam reforming on Cu/ZnO/Al2O3 catalysts. Part 2. A comprehensive kinetic model. *Applied Catalysis A: General*, *179*(1–2), 31–49. https://doi.org/10.1016/S0926-860X(98)00299-3

Peppley, B. A., Amphlett, J. C., Kearns, L. M., & Mann, R. F. (1999b). Methanol-steam reforming on Cu/Zno/Al2O3. Part 1: The reaction network. *Applied Catalysis A: General*, *179*(1–2), 21–29. https://doi.org/10.1016/S0926-860X(98)00298-1

Rosli, R. E., Sulong, A. B., Daud, W. R. W., Zulkifley, M. A., Husaini, T., Rosli, M. I., Majlan, E. H., & Haque, M. A. (2017). A review of high-temperature proton exchange membrane fuel cell (HT-PEMFC) system. *International Journal of Hydrogen Energy*, *42*(14), 9293–9314. https://doi.org/10.1016/j.ijhydene.2016.06.211

Seo, Y., You, H., Lee, S., Huh, C., & Chang, D. (2015). Evaluation of CO2 liquefaction processes for ship-based carbon capture and storage (CCS) in terms of life cycle cost (LCC) considering availability. *International Journal of Greenhouse Gas Control*, *35*, 1–12. https://doi.org/10.1016/j.ijggc.2015.01.006

Stangeland, K., Li, H., & Yu, Z. (2018). Thermodynamic Analysis of Chemical and Phase Equilibria in CO2 Hydrogenation to Methanol, Dimethyl Ether, and Higher Alcohols. *Industrial and Engineering Chemistry Research*, *57*(11), 4081–4094. https://doi.org/10.1021/acs.iecr.7b04866

Tronstad, T., Haugom, H. H., Haugom, G. P., & Langfeldt, L. (2017). Study on the use of fuel cells in shipping. *EMSA European Maritime Safety Agency*.

UNFCCC. (n.d.). *The Paris Agreement*. Retrieved May 24, 2021, from https://unfccc.int/process-and-meetings/the-paris-agreement/the-paris-agreement

Valdés-López, V. F., Mason, T., Shearing, P. R., & Brett, D. J. L. (2020). Carbon monoxide poisoning and mitigation strategies for polymer electrolyte membrane fuel cells – A review. *Progress in Energy and Combustion Science*, *79*. https://doi.org/10.1016/j.pecs.2020.100842

van Biert, L., Godjevac, M., Visser, K., & Aravind, P. v. (2016). A review of fuel cell systems for maritime applications. *Journal of Power Sources*, *327*(X), 345–364. https://doi.org/10.1016/j.jpowsour.2016.07.007

van Biert, L., Visser, K., & Aravind, P. v. (2020). A comparison of steam reforming concepts in solid oxide fuel cell systems. *Applied Energy*, *264*(February), 114748. https://doi.org/10.1016/j.apenergy.2020.114748

Wermuth, N., Lackner, M., Barnstedt, D., Zelenka, J., & Wimmer, A. (2020). *The HyMethShip Project: Innovative Emission Free Propulsion for Maritime Applications*. *X*, 1–14.

Wermuth, N., Zelenka, J., Moeyaert, P., Aul, A., & Borgh, M. (2020). The HyMethShip concept: Overview, concept development and obstacles for concept application in ocean-going vessel. *8th Transport Research Arena TRA*, *x*. www.hymethship.com.

Xu, Q., Xia, L., He, Q., Guo, Z., & Ni, M. (2021). Thermo-electrochemical modelling of high temperature methanol-fuelled solid oxide fuel cells. *Applied Energy*, *291*(March), 116832. https://doi.org/10.1016/j.apenergy.2021.116832

Zerbinati, O. (2002). A direct methanol fuel cell. *Journal of Chemical Education*, *79*(7), 829. https://doi.org/10.1021/ed079p829